Interacting domain walls and the five-vertex model

Jae Dong Noh and Doochul Kim
Department of Physics and Center for Theoretical Physics, Seoul National University, Seoul 151-742, Korea
(Received 30 August 1993)

We investigate the thermodynamic and critical properties of an interacting-domain-wall model which is derived from the triangular-lattice antiferromagnetic Ising model with the anisotropic nearest- and next-nearest-neighbor interactions. The model is equivalent to the general five-vertex model. Diagonalizing the transfer matrix exactly by the Bethe Ansatz method, we obtain the phase diagram displaying the commensurate and incommensurate (IC) phases separated by the Pokrovsky-Talapov transitions. The phase diagram exhibits commensurate phases where the domain-wall density q is locked at the values of 0, $\frac{1}{2}$, and 1. The IC phase is a critical state described by the Gaussian fixed point. The effective Gaussian coupling constant is obtained analytically and numerically for the IC phase using the finite-size-scaling predictions of the conformal-field theory. It takes the value $\frac{1}{2}$ in the noninteracting limit and also at the boundaries of $q = 0$ or 1 phase and the value 2 at the boundary of $q = \frac{1}{2}$ phase, while it varies smoothly throughout the IC region.

PACS number(s): 05.50.+q, 05.70.Jk, 64.60.Fr, 64.70.Rh

I. INTRODUCTION

There has been much interest in the two-dimensional statistical-mechanical systems which exhibit modulated phases on the periodic substrate [1]. Among those systems are monolayers of physisorbed gas on solid surface which display *incommensurate* (IC) and *commensurate* (C) phases. In the domain-wall description of IC phases [2], domain walls separating commensurate patches are considered as the basic fluctuating degrees of freedom. The domain walls can be arranged either parallel to each other (striped domain wall) or in hexagonal pattern (honeycomb domain wall) depending on the domain-wall crossing energy [3]. The simplest type of commensurate-incommensurate (C-IC) transition is the Pokrovsky–Talapov (PT) transition [4] which describes the transition into striped IC phase. Here, the fluctuations of the striped domain wall cause an effective repulsive interaction between walls. The interaction varies as $1/l^3$ if l is the average distance between walls. Due to this repulsive interaction between domain walls, the C–IC transition to the striped IC phase is a continuous transition with the specific-heat exponent $\alpha = 1/2$ and the domain-wall density displays a square-root dependence on the chemical potential of domain wall if we approach the phase boundary from the incommensurate side. The theory is explicitly realized in fermion models of striped IC phases where domain walls are represented as world lines of fermions living in a one-dimensional chain. A free-fermion model is also obtained as a low temperature approximation to the anisotropic next-nearest-neighbor Ising (ANNNI) model [5]. In these models, the IC phase is a critical phase where the correlation functions decay by the power laws of the distance rather than by the exponential function of the distance. Recently, Park and Widom showed that the IC phase modeled by the free-fermion Hamiltonian is described in the continuum limit by the Gaussian model with the coupling constant $g = 1/2$ by an explicit calculation of the toroidal partition function [6]. The effect of domain-wall interaction has also been studied in the fermion model derived from an approximation to the ANNNI model [7] and in a phenomenological model [6].

In this paper, we consider an exactly solvable *interacting* domain-wall model derived from the triangular-lattice antiferromagnetic Ising model (TAFIM). It is well known that the TAFIM with only nearest-neighbor coupling has infinitely degenerate ground states due to frustration on each elementary triangle. Each ground state can be mapped into a configuration of covering the plane by three types of diamonds. Blöte and Hilhorst [8] introduced a solid-on-solid model derived from these configurations. Regarding two types of diamonds as domain-wall excitations, one also obtains a striped domain-wall configuration. Blöte and Hilhorst [8] utilized this connection to obtain exact solution to the noninteracting domain-wall problem. As the fugacities of walls change, there is a phase transition from an ordered phase to the critically disordered phase which is described by the Gaussian fixed point with the coupling constant $g = 2$. The nature of the transition is found to be that of the PT transition [4]. Nienhuis, Hilhorst, and Blöte [9] identified various spin-wave and vortex operators of the Gaussian model in terms of the solid-on-solid model and argued that infinitesimal next-nearest-neighbor (NNN) interactions and magnetic field in TAFIM would change the coupling constant g of the Gaussian model. From this they suggested a schematic phase diagram in the parameter space composed of the nearest-neighbor interactions, the NNN interactions and the external magnetic field. More recently the effect of the external magnetic field on g has been studied by Blöte *et al.* [10] and the behaviors predicted in Ref. [9] is confirmed.

We show in Sec. II that the ground-state configurations of the TAFIM under the general boundary conditions are equivalent to the striped domain-wall configurations.

When the NNN interactions in the TAFIM are turned on in an anisotropic manner, they correspond to extra energies between adjacent domain walls. Only the same types of walls can touch each other and there are two types of wall interactions. We also show in Sec. II that the striped domain-wall configuration is exactly mapped to the arrow configuration of the five-vertex model. But, if both types of wall interactions are present, the Boltzmann weight cannot be represented by a product of vertex weights. However, when only one type of domain walls interact with each other, it can be written as a product of vertex weights and the partially interacting domain-wall model reduces to the general five-vertex model.

In Sec. III, we diagonalize the transfer matrix of the five-vertex model using the Bethe Ansatz method. We develop Bethe ansatz solutions both for domain walls and domain-wall holes. From these solutions, we obtain a full phase diagram of the partially interacting model. The phase diagram displays the C and IC phases separated by the PT transition and the first order transition. It also exhibits a new commensurate phase where the domain-wall density is locked to the value $1/2$ for a range of the chemical potential of the wall. This phase does not appear in the noninteracting domain-wall models and is a feature resulting from the domain-wall interactions. This is akin to the antiferromagnetically ordered phase of the ANNNI model.

In Sec. IV, we investigate the critical properties of the IC phase. It is shown that the interaction between domain walls causes a continuous variation of the coupling constant g of the Gaussian model resulting in nonuniversal critical behaviors. It is studied by analytic perturbative calculations and numerical calculations. We discuss and summarize our result in Sec. V and present discussions on the Yang–Baxter equation and the calculation of the modular covariant partition functions of the $T = 0$ TAFIM under the general boundary conditions in Appendixes A and B, respectively.

II. TRANSFER MATRIX FORMULATION OF INTERACTING DOMAIN-WALL MODEL

We write the Hamiltonian $\mathcal{H}$ including $1/kT$ of the TAFIM with the nearest- and next-nearest-neighbor interaction as

$$\mathcal{H} = -\sum_{\langle ij\rangle}(K+\delta_a)s_i s_j - \sum_{\langle\langle ij\rangle\rangle}{}'\varepsilon_a s_i s_j - K\mathcal{N}, \qquad (1)$$

where $s_i = \pm 1$ is an Ising spin variable at site i, the first (second) sum is over the nearest (next nearest) neighbor pairs of sites, $K+\delta_a$ (ε_a), $a = 1,2,3$, are the anisotropic nearest (next nearest) neighbor couplings whose index a depends on the direction of the bond $\langle ij\rangle$ ($\langle\langle ij\rangle\rangle$) as shown in Fig. 1(a), and finally $\mathcal{N}$ is the number of lattice sites.

Monte Carlo simulation and other studies [11,12] show that this system has rich critical phenomena in the full parameter space. But, we will only consider the zero-temperature limit of this system. By the zero-temperature limit, we actually mean the infinite-coupling limit $K \to -\infty$ leaving δ_j's and ε_j's finite. Equation (1) in this limit will be called the $T = 0$ TAFIM. Here, only those configurations which have precisely one pair of parallel spins around each elementary triangle are energetically allowed. Though this imposes much restriction on the spin configurations, it is important to study this limiting case because the $T = 0$ TAFIM is equivalent to many interesting problems, e.g., the diamond and/or dimer covering problem [8] and the triangular solid-on-solid model [9,13]. Moreover, the $T \neq 0$ behavior of the TAFIM can be inferred from the $T = 0$ behavior.

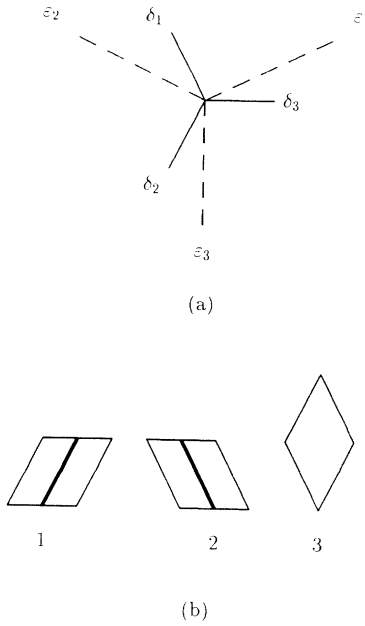

FIG. 1. (a) Correspondence between the anisotropic couplings and the lattice directions in the TAFIM with nearest- and next-nearest-neighbor interactions. (b) Labeling of three types of diamonds. Types 1 and 2 are considered as domain-wall excitations.

Here, we will show that the $T = 0$ TAFIM with NNN interactions is equivalent to the interacting striped domain-wall model where the NNN interaction ε_j ($j = 1,2$) plays the role of wall-wall interactions. If we draw lines between all nearest-neighbor pairs of antiparallel spins for a given ground-state configuration of the TAFIM, the resulting configuration is that of a covering of the plane by diamonds. Figure 2 shows a typical TAFIM ground state and its corresponding diamond covering configuration. The three types of diamonds are called types 1, 2, and 3, respectively as shown in Fig. 1(b). Strictly speaking, there is two-to-one correspondence because of the global spin-reversal symmetry of the TAFIM in the absence of magnetic field.

From a diamond covering configuration, a striped domain-wall configuration is obtained by regarding the diamonds of types 1 and 2 as domain-wall excitations. Type-3 diamonds are regarded as the vacuum. Thick lines on the faces of types 1 and 2 diamonds in Fig. 1(b) and Fig. 2 visualize the domain walls. A section of domain walls which is obtained from the diamond of types 1 and 2 will be called the domain wall of types 1 and 2, respectively. Two walls are defined to be interacting

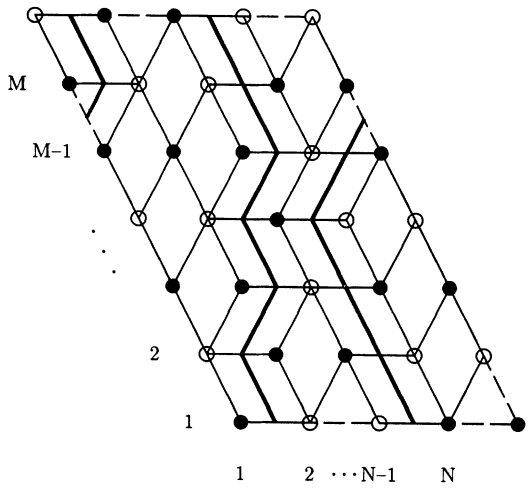

FIG. 2. A typical striped domain-wall configuration derived from a ground state of the TAFIM on a 4×6 lattice. The filled circles represent spin up states and empty circles represent spin down states. We use the periodic boundary condition along the horizontal direction and the antiperiodic boundary condition along the vertical direction. So, the resulting domain-wall configuration has even Q and odd Ω.

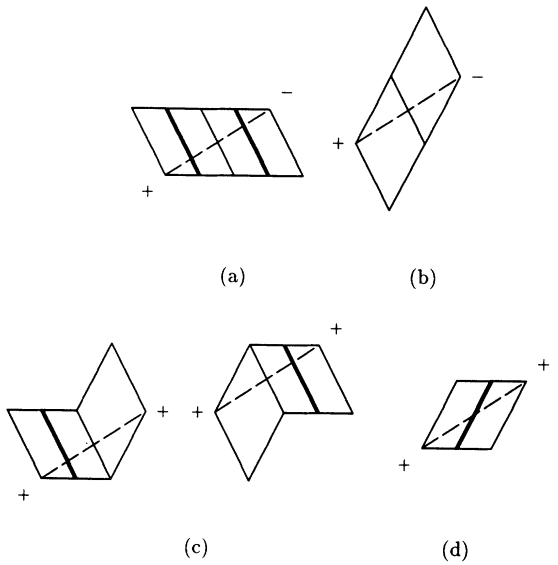

FIG. 3. Four possibilities of next-nearest-neighbor bonds along the direction 1.

when their sides touch each other. The thermodynamic parameters which control the equilibrium property of interacting striped domain-wall system are the fugacities x_1 and x_2 of domain walls of types 1 and 2, respectively, and the fugacities y_1 and y_2 for each pair of adjacent domain walls of types 1 and 2, respectively. Note that different types of domain walls cannot be adjacent. The partition function $\mathcal{Z}_{\text{d.w.}}$ for the interacting domain-wall model is

$$\mathcal{Z}_{\text{d.w.}} = \sum x_1^{n_1} x_2^{n_2} y_1^{l_1} y_2^{l_2}, \tag{2}$$

where the summation is taken over all striped domain-wall configurations and n_i is the total length of domain wall of type i and l_i is the total number of incidents where domain walls of type i touch each other and share a side, i.e., the number of wall-wall interactions of type i.

When $\varepsilon_3 = 0$ in Eq. (1), the energy of the $T = 0$ TAFIM can be written in terms of n_i and l_i. Nearest-neighbor interactions contribute [8] simply

$$\sum_{i=1,2,3} (-\delta_i + \delta_j + \delta_k) n_i,$$

where (i,j,k) is the cyclic permutation of $(1,2,3)$ and $n_3 = \mathcal{N} - n_1 - n_2$ is the total number of type-3 diamonds. From now on we set $\delta_3 = 0$ without loss of generality. To relate the NNN interaction energies to l_i, consider first the bonds connecting NNN pair of sites along the direction 1. [See Fig. 1(a).] They cross either (a) two type-2 domain walls or (b) two type-3 diamonds or (c) one type-2 wall and one type-3 diamond or (d) one type-1 domain wall. These possibilities are shown in Fig. 3. If we let n_a, n_b, n_c and n_d be the number of cases (a), (b), (c) and (d), respectively, the bonds contribute $\varepsilon_1(n_a + n_b - n_c - n_d)$ to the energy. But one can easily identify $n_d = n_1$ and $n_a = l_2$. Moreover each of type-2 walls is crossed by two NNN bonds so that it appears twice in the list of Fig. 3 while the total number of type-2 walls counted in Fig. 3 is $2n_a + n_c$. Thus $2n_2 = 2n_a + n_c$. These relations, together with the sum rule $n_a + n_b + n_c + n_d = \mathcal{N}$, give the energy

$$\varepsilon_1(\mathcal{N} + 4l_2 - 4n_2 - 2n_1) \quad .$$

Similar counting holds for NNN bonds along the direction 2.

Putting these together, the ground-state energy of Eq. (1) for $\varepsilon_3 = 0$ becomes

$$\begin{aligned} E_0 = &-2(\delta_1 + \varepsilon_1 + 2\varepsilon_2)n_1 - 2(\delta_2 + \varepsilon_2 + 2\varepsilon_1)n_2 \\ &+4\varepsilon_2 l_1 + 4\varepsilon_1 l_2 + \mathcal{N}(\delta_1 + \delta_2 + \varepsilon_1 + \varepsilon_2) \quad . \end{aligned} \tag{3}$$

Thus the fugacities for the interacting domain-wall model are related to anisotropic coupling energies of the TAFIM model as

$$\begin{aligned} x_1 &= \exp[2(\delta_1 - \delta_3) + 2\varepsilon_1 + 4\varepsilon_2], \\ x_2 &= \exp[2(\delta_2 - \delta_3) + 2\varepsilon_2 + 4\varepsilon_1], \\ y_1 &= \exp[-4\varepsilon_2], \\ y_2 &= \exp[-4\varepsilon_1]. \end{aligned} \tag{4}$$

Next, we show that to each striped domain-wall configuration, one can assign a vertex configuration. To do this we deform the triangular lattice into the square one as shown in Fig. 4. One then finds that there are five types of unit squares. Figure 5 shows them together with assignment of vertex configurations. If one works under the ice rule, the assignment of vertices shown in Fig. 5 is unique modulo the arrow reversal.

In this way, we obtain one-to-one correspondence between striped domain-wall configurations and bond-arrow configurations satisfying the ice rule. Vertical up arrow indicates the presence of a domain wall. In the

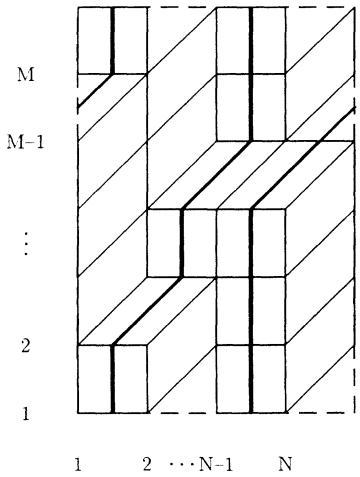

FIG. 4. Deformation of Fig. 2 into a square lattice.

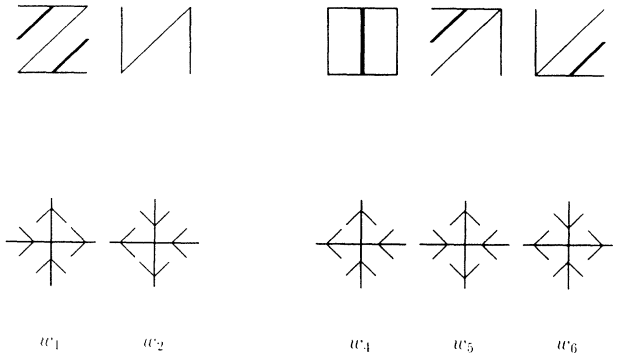

FIG. 5. Five types of unit squares in the deformed lattice and assignment of vertex configurations.

TAFIM language, vertical up arrows correspond to horizontal nearest-neighbor spin pairs which have opposite signs and right arrows correspond to vertical nearest-neighbor spin pairs which have the same signs. The absence of the third vertex (or the fourth upon arrow reversal) is a result of our deforming the triangular lattice in the manner shown in Fig. 4. If it were deformed in the opposite direction, it is the first vertex (or the second upon the arrow reversal) which does not appear. In any case, one obtains the five-vertex-model configurations.

The five-vertex model on the square lattice is obtained from the six-vertex-model by suppressing one of the first four vertices. The five-vertex model with special choice of its vertex weights was first considered by Wu [14] as a limiting case of the six-vertex model and is studied in connection with the nonintersecting directed random walk [15] and the directed percolation problem in three dimension [16]. Recently, Gulácsi *et al.* [17] studied its phase diagram for a special case. The general five-vertex model is obtained by assigning arbitrary vertex weights to each type of vertices but there are only three independent parameters since the vertices 5 and 6 always occur in pairs along a row under the periodic boundary condition and a global rescaling of weights introduces only a trivial factor.

The partition function $\mathcal{Z}_{5\text{-}v}$ of the five-vertex model is

$$\mathcal{Z}_{5\text{-}v} = \sum w_1^{N_1} w_2^{N_2} w_4^{N_4} w_5^{N_5} w_6^{N_6}, \tag{5}$$

where the summation is taken over all arrow configurations and N_i is the number of the ith vertex appearing in an arrow configuration. Unfortunately, if we assign the Boltzmann weight of an arrow configuration as a product of local vertex weights, we cannot treat the fully interacting domain-wall model ($\varepsilon_1 \neq 0, \varepsilon_2 \neq 0$ case). However, if we restrict ourselves to the special case $\varepsilon_1 = 0$ ($y_2 = 1$), then Eq. (2) can be expressed in the form of Eq. (5). From now on, we consider the partially interacting model where only domain walls of type 1 interact.

The vertex of type 1 represents the case where the two domain walls of type 1 are interacting. So, if we choose vertex weights as

$$\begin{aligned} w_1 &= x_1 y_1, \\ w_2 &= 1, \\ w_4 &= x_2, \\ w_5 = w_6 &= \sqrt{x_1}, \end{aligned} \tag{6}$$

the partition function $\mathcal{Z}_{5\text{-}v}$ becomes the same as that of the partially interacting domain-wall system:

$$\mathcal{Z}_{5\text{-}v} = \sum x_1^{n_1} x_2^{n_2} y_1^{l_1} \quad . \tag{7}$$

We study the five-vertex model using the transfer matrix. Suppose the lattice has M rows and N columns, and periodic boundary conditions are imposed in both directions. Let $\boldsymbol{\alpha} = (\alpha_1, \ldots, \alpha_N)$ denote the state of vertical arrows of one row. Then, as usual, we can write the partition function $\mathcal{Z}_{5\text{-}v}$ as

$$\mathcal{Z}_{5\text{-}v} = \mathrm{Tr}\ \mathbf{T}_{5\text{-}v}^M \tag{8}$$

where $\mathbf{T}_{5\text{-}v}$ is the 2^N by 2^N transfer matrix with elements

$$\mathbf{T}_{5\text{-}v}(\boldsymbol{\alpha}, \boldsymbol{\beta}) = \sum_{\{\mu_i = \pm 1\}} \prod_{i=1}^{N} W(\mu_i, \alpha_i | \beta_i, \mu_{i+1}) \quad . \tag{9}$$

In Eq. (9), $W(\mu, \alpha | \beta, \nu)$ is the weight of the vertex configuration in the standard notation [18]. Let $\mathbf{T}_L$ ($\mathbf{T}_R$) be the transfer matrix of the five-vertex model with the first horizontal arrow fixed to the left (right). This can be written graphically as

$\mathbf{T}_L(\boldsymbol{\alpha} \mid \boldsymbol{\beta}) =$ 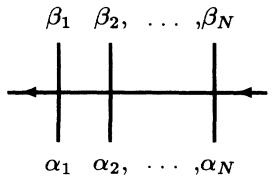

$\mathbf{T}_R(\boldsymbol{\alpha} \mid \boldsymbol{\beta}) =$ 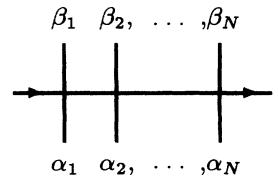

Then the transfer matrix can be written as

$$\mathbf{T}_{5\text{-}v} = \mathbf{T}_R + \mathbf{T}_L \quad . \tag{10}$$

From the ice rule, the number of up arrows on a row and right arrows on a column are conserved. In the language of domain wall, the number of up arrows per row corresponds to the number of domain walls per row and the number of right arrows per column corresponds to the number of type-1 domain walls per column. We will call them Q and Ω, respectively. From the conservation of Q, $\mathbf{T}_{5\text{-}v}$ is a direct sum of submatrices labeled by Q which only act on the subspace with Q domain walls. Thus,

$$\mathbf{T}_{5\text{-}v} = \bigoplus_{Q=0,\ldots,N} (\mathbf{T}_{R,Q} + \mathbf{T}_{L,Q}), \tag{11}$$

where $\bigoplus$ stands for the direct sum and $\mathbf{T}_{R,Q}$ ($\mathbf{T}_{L,Q}$) denotes the sector Q of $\mathbf{T}_R$ ($\mathbf{T}_L$).

The partition function $\mathcal{Z}_{5\text{-}v}$ of the five-vertex model is obtained from the partition function $\mathcal{Z}_{\rm TAFIM}$ of the $T = 0$ TAFIM as follow. Suppose the triangular lattice has M rows and N columns as in Fig. 2 under the boundary condition (μ, ν) defined by

$$\begin{aligned} s_{i,M+1} &= (-1)^{\mu} s_{i,1} \qquad (\mu = 0,1), \\ s_{N+1,j} &= (-1)^{\nu} s_{1,j} \qquad (\nu = 0,1), \end{aligned} \tag{12}$$

where μ, ν are 0 (1) for periodic (antiperiodic) boundary condition. Let $\boldsymbol{s} = (s_1, \ldots, s_N)$ denote the spin state of one row. It can also be represented by $(s_1, \boldsymbol{\alpha})$ where $\boldsymbol{\alpha} = (\alpha_1, \ldots, \alpha_N)$ and $\alpha_i = -s_i s_{i+1}$. With the identification of $\alpha = 1$ (-1) to the up (down) arrow in the ith vertical bond in the dual lattice, one notes that $\boldsymbol{\alpha}$ is the arrow configuration of a row of vertical bonds of the corresponding five-vertex-model configuration. The transfer matrix $\mathbf{T}^{(\nu)}_{\rm TAFIM}$ of the $T = 0$ TAFIM is defined through its matrix element $\mathbf{T}^{(\nu)}_{\rm TAFIM}(s_1, \boldsymbol{\alpha} \mid s_1', \boldsymbol{\alpha}')$ which is the Boltzmann weight for two successive row configurations $(s_1, \boldsymbol{\alpha})$ and $(s_1', \boldsymbol{\alpha}')$ with the boundary condition ν along the horizontal direction. Due to the global spin-reversal symmetry, it takes the block form

$$\begin{aligned} \mathbf{T}^{(\nu)}_{\rm TAFIM} &= \begin{pmatrix} \mathbf{T}_{++} & \mathbf{T}_{+-} \\ \mathbf{T}_{-+} & \mathbf{T}_{--} \end{pmatrix} \\ &\sim \begin{pmatrix} \mathbf{T}_{++} + \mathbf{T}_{+-} & 0 \\ 0 & \mathbf{T}_{++} - \mathbf{T}_{+-} \end{pmatrix}, \end{aligned} \tag{13}$$

where $\mathbf{T}_{ss'}$ $(s, s' = \pm)$ is the matrix whose elements are $\mathbf{T}^{(\nu)}_{\rm TAFIM}(s, \boldsymbol{\alpha} \mid s', \boldsymbol{\alpha}')$ and $\sim$ denotes an equivalence up to the similarity transformation. We use the fact that $\mathbf{T}_{ss'} = \mathbf{T}_{-s-s'}$. If we denote the partition function of the $T = 0$ TAFIM under the boundary condition (μ, ν) as $\mathcal{Z}^{(\mu,\nu)}_{\rm TAFIM}$, it can be written as

$$\mathcal{Z}^{(\nu,\mu)}_{\rm TAFIM} = {\rm Tr}\, \mathbf{R}^{\mu} \left[\mathbf{T}^{(\nu)}_{\rm TAFIM}\right]^M, \tag{14}$$

where $\mathbf{R}$ is the spin-reversal operator.

Since the sign of the spin reverses by crossing each domain wall in the horizontal direction, spin configurations under the boundary condition $\nu = 0$ (1) yield only domain-wall configurations with Q even (odd). Therefore, $\mathbf{T}_{++}$ and $\mathbf{T}_{+-}$ in Eq. (13) are $\mathbf{T}_R$ and $\mathbf{T}_L$, respectively, of the five-vertex model restricted to Q even (odd) sectors for $\nu = 0$ (1). This shows that the transfer matrix spectra of the two models are not identical. Only the even or odd Q sector of Eq. (11) are present in Eq. (13) while the latter includes the block $\mathbf{T}_{++} - \mathbf{T}_{+-}$ which is not present in the five-vertex model. And the spin configurations under the boundary condition $\mu = 0$ (1) yield only domain-wall configurations with Ω even (odd) assuming that M is even, since the sign of spin changes in every step except when crossing a type-1 domain wall in the vertical direction. If M is odd, even (odd) Ω corresponds to $\mu = 1$ (0). So, the partition function $\mathcal{Z}_{5\text{-}v}$ of the five-vertex model is given by

$$\mathcal{Z}_{5\text{-}v} = \frac{1}{2}\left(\mathcal{Z}^{(0,0)}_{\rm TAFIM} + \mathcal{Z}^{(0,1)}_{\rm TAFIM} + \mathcal{Z}^{(0,1)}_{\rm TAFIM} + \mathcal{Z}^{(1,1)}_{\rm TAFIM}\right), \tag{15}$$

where the factor 1/2 accounts for the two-to-one correspondence. This relation will be used in Sec. IV to obtain the toroidal partition function $\widetilde{\mathcal{Z}}_{5\text{-}v}$ of the five-vertex model.

III. PHASE DIAGRAM

The five-vertex-model transfer matrix can be diagonalized by the Bethe ansatz method as a special case of the general six-vertex model [14]. Its phase diagram has recently been calculated by Gulácsi, Beijeren, and Levi [17] for the special case of $w_1 = w_2$. (Gulácsi, Beijeren, and Levi use the notation $w_2 = 0$. Their work and ours are related by the transformation $w_1 \leftrightarrow w_4, w_2 \leftrightarrow w_3$ and $w_5 \leftrightarrow w_6$.) In this section, we generalize it to the full three-dimensional parameter space and also calculate the domain-wall densities. We also discuss types of solutions of the Bethe ansatz equation (BAE) of the five-vertex model.

The eigenvalues of the transfer matrix Eq. (9) in the sector Q $(\neq N)$ are given by [14,17]

$$\Lambda_Q = w_2^{N-Q} w_4^Q \prod_{j=1}^{Q} \left(1 + \frac{w_5 w_6}{w_2 w_4} z_j\right), \tag{16}$$

where the set $\{z_1, z_2, \ldots, z_Q\}$ are the solutions of the BAE

$$z_j^N = (-1)^{Q-1} \prod_{l=1}^{Q} \frac{1 - \Delta z_j}{1 - \Delta z_l} \quad , \quad j = 1, 2, \ldots, Q \tag{17}$$

with

$$\Delta = \frac{w_1 w_2 - w_5 w_6}{w_2 w_4} \quad . \tag{18}$$

All z_j's should be distinct. When $Q = N$, $\Lambda_N = w_1^N + w_4^N$.

An alternative expression for the eigenvalue which is useful for $Q > N/2$ is given by

$$\Lambda_Q = w_1^Q \prod_{j=1}^{\bar{Q}} \left\{ \frac{w_5 w_6}{w_1 z_j - w_4} \right\} + w_4^Q \prod_{j=1}^{\bar{Q}} \left\{ w_2 - \frac{w_5 w_6 z_j}{w_1 z_j - w_4} \right\}, \quad (19)$$

where $\bar{Q} \equiv N - Q$ is the number of domain-wall holes and the set $\{z_1, z_2, \ldots, z_{\bar{Q}}\}$ is again given by Eq. (17) with Q replaced by $\bar{Q}$. We call Eq. (16) and Eq. (19) the domain-wall representation and the domain-wall hole representation, respectively. Using Eq. (6) into Eqs. (16), (18), and (19) gives Λ_Q in terms of the domain-wall parameters as

$$\Lambda_Q = x_2^Q \prod_{j=1}^{Q} (1 + a z_j) \quad (20)$$

or

$$\Lambda_Q = x_2^Q (\Delta + a)^Q \prod_{j=1}^{\bar{Q}} \left\{ \frac{a}{(\Delta + a) z_j - 1} \right\} + x_2^Q \prod_{j=1}^{\bar{Q}} \left\{ 1 - \frac{a z_j}{(\Delta + a) z_j - 1} \right\}, \quad (21)$$

where a is the ratio of two domain-wall fugacities

$$a = x_1 / x_2 \quad (22)$$

and

$$\Delta = x_1 (y_1 - 1)/x_2 = a(y_1 - 1) \quad . \quad (23)$$

We will call Δ the interaction parameter. It is positive for attractive interaction and negative for repulsive interaction between domain walls.

Defining the momenta $\{p_j\}$ by $z_j = e^{i p_j}$, Eq. (17) also takes the familiar form

$$N p_j = 2\pi I_j + \sum_{l=1}^{Q} \Theta(p_j, p_l), \quad (24)$$

where

$$e^{i\Theta(p,q)} \equiv -\frac{1 - \Delta e^{ip}}{1 - \Delta e^{iq}} \quad (25)$$

and I_j's are half-integers for even Q and integers for odd Q ranging from $-(N-1)/2$ to $(N-1)/2$. Different eigenvalues come from different choices of the set $\{I_j\}$.

The BAE may take another form. If we define

$$s = \frac{1}{Q} \sum_l \ln(1 - \Delta z_l) \quad , \quad (26)$$

then the BAE becomes

$$z_j = (-1)^{(Q-1)/N} (1 - \Delta z_j)^q e^{-qs}, \quad (27)$$

where $q = Q/N$ is the domain-wall density. This equation gives z_j's as a function of s which should, in turn, be determined from its defining Eq. (26).

Note that the BAE [Eq. (17)] arises from the periodic boundary condition on the wave function of $\mathbf{T}_{5\text{-}v}$ [19]. It is also interesting to consider another boundary condition, say, the antiperiodic boundary condition. The effect of the boundary condition is to shift domain walls out of the Nth site to the first site with appropriate phase factor 1 (-1) for periodic (antiperiodic) boundary condition. The shift operation is done by the operator $\mathbf{T}_R$. So, if we impose antiperiodic boundary condition, the resulting matrix we diagonalize is $\mathbf{T}_L - \mathbf{T}_R$. In this case, the expression for eigenvalues remains the same except for the fact that I_j should be integers for even Q and half-integers for odd Q. So, we can obtain whole spectrum of the transfer matrix of the $T = 0$ TAFIM from the transfer matrix of the five-vertex model under periodic and antiperiodic boundary conditions. Note that the antiperiodic boundary condition here is different from that which reverses the sense of horizontal arrows.

The free energy in the language of the domain-wall physics is a function of x_1, x_2 and y_1 through Eq. (6). From now on, we regard it as a function of Δ, x_2 and $a = x_1/x_2$. Since the free energy is given by the maximum eigenvalue of the transfer matrix, $f(x_2, a, \Delta)$, the free energy per site in the units of kT, is written in the form

$$f(x_2, a, \Delta) = -\lim_{N\to\infty} \max_Q \left[\frac{1}{N} \ln \Lambda_Q \right] = -\max_q [q \ln x_2 + \kappa(q)], \quad (28)$$

where $\kappa(q)$, which will be called the configurational free energy, is given by

$$\kappa(q) = \lim_{N\to\infty} \max_{\{z_j\}} \left[\frac{1}{N} \sum_{j=1}^{Q} \ln(1 + a z_j) \right] \quad . \quad (29)$$

Here, $\{z_j\}$'s are the solutions of the BAE. The equation of state which relates the equilibrium domain-wall density q as a function of thermodynamic parameters is given by the relation

$$q(x_2, a, \Delta) = \frac{Q_0}{N}, \quad (30)$$

where Q_0 is the value of Q at which Λ_Q attains the maximum value. The equation of state can be rewritten as

$$\frac{\partial}{\partial q} \kappa(q, a, \Delta) = -\ln x_2 \quad (31)$$

if $\kappa(q)$ is a differentiable and convex function. The configurational free energy $\kappa(q)$ is a Legendre transformation of f. That is, it is a free energy as a function of domain-wall density while f is a free energy as a function of the domain-wall fugacity.

We now classify types of solutions of the BAE corresponding to the maximum eigenvalue. First, consider the case $-1 < \Delta < 1$. This region contains the noninteracting case with $\Delta = 0$ which is consid-

ered in [14]. In this case, the Θ function defined in Eq. (25) is identically 0. So, any set $\{I_j\}$ of Q different numbers are solutions of the BAE and the solution giving the maximum value of Λ_Q is $\{I_j\} = \{-(Q-1)/2, -(Q-1)/2+1, \ldots, (Q-1)/2\}$. We assume that this set $\{I_j\}$ still gives the maximum eigenvalue even after the turning-on of weak interaction and remains so in the whole region $-1 < \Delta < 1$. This assumption is tested by direct numerical diagonalization of the transfer matrix with N up to 15. We call this type of solution as the *free magnon type.*

When $|\Delta| > 1$, there appear other types of solutions. Assume that the solution is of the form

$$\begin{aligned} z_j &= \Delta^{b_j}\bar{z}_j, \quad j = 1, \ldots, N_+ \\ z_j &= \bar{z}_j, \quad j = (N_+{+}1), \ldots, (N_+{+}N_0) \\ z_j &= \frac{1}{\Delta} - \frac{\bar{z}_j}{\Delta^{1+a_j}}, \quad j = (N_+{+}N_0+1), \ldots, Q, \end{aligned} \tag{32}$$

where a_j and b_j are constants greater than 0 and $\bar{z}_j$'s are assumed to remain of order 1 as $|\Delta| \to \infty$. In other words, of Q z_j's, N_+ are diverging, N_0 remain finite, and $N_- = Q-(N_+{+}N_0)$ vanish inversely as $|\Delta| \to \infty$. Then, the necessary condition that this set should be a solution of the BAE is either (i) $N_+ = N_- = 0$ so that all z_j's are of order 1 or (ii) $N_0 = 0, b_j = (Q - N_+)/N_+$ and $a_j = (N-Q)/N_+$. We also call the first type as the *free magnon type* while the second type will be called as the *bounded magnon type.* Of these possibilities, one can easily show that the configurational free energy is realized by the *free magnon type* if $\Delta \to -\infty$ and the *bounded magnon type* with $N_+ = 1$ if $\Delta \to \infty$. We find numerically that this feature also persists for all Δ in the range $|\Delta| > 1$.

It is very difficult to obtain the equation of state [Eq. (31)] analytically for whole range of parameters x_2, a, and Δ. But, the phase boundaries which separate the commensurate phases with domain-wall density 0 or 1 from the incommensurate phase can be obtained if we solve the BAE in the $q \to 0$ or 1 limit. Apart from the C phases with domain-wall density 0 or 1, there appears a new C phase with $q = 1/2$ if a is large so that Δ can take values less than some critical value Δ_c. (Below, we will see that Δ_c takes the value -4.) Consider the case where domain walls of type 1 are much more favorable to form than those of type 2 ($a = x_1/x_2 \gg 1$) and there are repulsive interaction between them ($y_1 < 1$) so that the interaction parameter Δ is less than Δ_c. Then, the most energetically favorable state for $q \le 1/2$ is the state where there are only type-1 domain walls with no adjacent pairs. But, if q is larger than $1/2$, there should appear type-2 walls and adjacent pairs of domain walls of type 1 whose energy costs are large. So, it is expected that there is a discontinuity in x_2 which controls the total number of domain walls across the $q = 1/2$ line. The phase boundary of the $q = 1/2$ C phase can be also determined analytically. Our results for the phase boundary are given by Eqs. (35), (38), (41), (49), (59), and (70) and are illustrated in Fig. 7.

(i) $\Delta < 1$, $q = 0$. In the region $\Delta < 1$, the *free magnon type* solution in the $q \to 0$ limit is

$$z_j = e^{i\theta_j}\left[1 + \frac{\Delta q}{1-\Delta}\left(1 - e^{i\theta_j}\right)\right] + O(q^3), \tag{33}$$

where $\theta_j = 2\pi I_j/N$ and $\{I_j\}$ is a set of integers or half-integers depending on the parity of the domain-wall number Q. The maximum value of $\kappa(q)$ is obtained if we choose the set $\{I_j\} = \{-(Q-1)/2, -(Q-1)/2+1, \ldots, (Q-1)/2\}$ and the next largest values of $\kappa(q)$ are obtained by using the set $\{I'_j = I_j + m\}$ which is a shift of the set $\{I_j\}$ by an integer m. With this solution, the configurational free energy κ is given from Eq. (29) by

$$\begin{aligned} \kappa(q) &= \frac{1}{2\pi}\int_{-\pi q}^{\pi q} \ln\left[1 + ae^{i\theta}\left(1 + \frac{\Delta q}{1-x}(1-e^{i\theta})\right)\right] d\theta \\ &\quad + O(q^4) \\ &= q\ln(1+a) - \frac{a\pi^2}{6(1+a)}q^3 + O(q^4) \quad . \end{aligned} \tag{34}$$

This, together with Eq. (31), implies that $q = 0$ if $x_2 \le 1/(1+a)$. Thus, we obtain the phase boundary $x_2 = x_{0C}$ between the $q = 0$ C phase and the IC phase as

$$x_{0C} = \frac{1}{1+a} \tag{35}$$

or equivalently $x_1 + x_2 = 1$. For x_2 slightly larger than x_{0C}, Eq. (34) gives

$$q \simeq \sqrt{\frac{2(1+a)}{a\pi^2}}\ (\ln x_2 - \ln x_{0C})^{1/2}. \tag{36}$$

The domain-wall density thus shows the square-root dependence on domain-wall formation energy which is the general character of the PT transition. This type of singularity is originated from the fact that the leading contribution $\kappa(q)$ aside from the linear term is of order q^3. It is originated from the entropy reduction due to the collision of domain walls [20].

(ii) $\Delta < 1$, $q = 1$. Next, consider the case near $q = 1$. In this case, it is easier to consider the BAE for domain-wall holes rather than domain walls. Inserting Eq. (33) with q replaced by $\bar{q}$ into Eq. (21), we obtain $\kappa(q)$ near $q = 1$. $\bar{q} = 1 - q$ is a domain-wall hole density. There are two cases to consider depending on whether $\Delta + a > 1$ or $\Delta + a < 1$. When $\Delta + a > 1$, the first term in the right-hand side of Eq. (21) dominates and hence

$$\begin{aligned} \kappa(q) &= q\ln(\Delta+a) + \frac{1}{N}\sum_{j=1}^{\bar{Q}} \ln\left[\frac{a}{(\Delta+a)z_j - 1}\right] \\ &= \ln(\Delta+a) - \bar{q}\ \ln\frac{(\Delta+a)(\Delta+a-1)}{a} \\ &\quad - \frac{\bar{q}^3}{6}\frac{\pi^2(\Delta+a)}{(\Delta+a-1)^2} + O(\bar{q}^4) \quad . \end{aligned} \tag{37}$$

From this, the phase boundary $x_2 = x_{1C}$ between the $q = 1$ C phase and the IC phase is given by

$$x_{1C} = \frac{a}{(\Delta+a)(\Delta+a-1)} \qquad (\Delta + a > 1) \tag{38}$$

and the equilibrium domain-wall density near x_{1C} is given by

$$q \simeq 1 - \sqrt{\frac{2(\Delta+a-1)^2}{\pi^2(\Delta+a)}}\,(\ln x_{1C} - \ln x_2)^{1/2} \quad . \tag{39}$$

Similarly, when $\Delta+a<1$, the configurational free energy is given by

$$\begin{aligned}\kappa(q) &= \frac{1}{N}\sum_{j=1}^{\bar{Q}} \ln\left[1 - \frac{a}{(\Delta+a)z_j - 1}\right] \\ &= \bar{q}\ln\frac{1-\Delta}{1-\Delta-a} - \frac{1}{6}\bar{q}^3\frac{a\pi^2(1-a\Delta-\Delta^2)}{(\Delta+a-1)^2(\Delta-1)^2} \\ &\quad + O(\bar{q}^4) \quad , \end{aligned} \tag{40}$$

from which the phase boundary $x_2 = x_{1c}$ and the equilibrium domain wall density near x_{1C} are given by

$$x_{1C} = \frac{1-\Delta}{1-\Delta-a} \qquad (\Delta+a<1) \tag{41}$$

and

$$q \simeq 1 - \sqrt{\frac{2(\Delta+a-1)^2(\Delta-1)^2}{a\pi^2(1-a\Delta-\Delta^2)}}\,(\ln x_{1c} - \ln x_2)^{1/2} \tag{42}$$

So, we conclude that when $\Delta<1$, there are commensurate phases with domain-wall density 0 for $x_2 < x_{0c}$ and domain-wall density 1 for $x_2 > x_{1c}$. In between, the equilibrium domain-wall density increases smoothly as x_2 increases as long as $\Delta > -4$. Figure 6 shows a typical x_2 dependence of q for the case of $a=1$. The curves are obtained numerically by solving the BAE for N up to 150. The case $\Delta<-4$ will be considered later.

(iii) $\Delta > 1$. Now, consider the case where there is a strong attractive interaction between domain walls so that $\Delta > 1$. The solution of the BAE maximizing κ is of the *bounded magnon type* with $N_+ = 1$. The exact solution of the BAE is easily obtained from the transformation of z to $\bar{z}$ defined by

$$\begin{aligned} z_1 &= \bar{z}_1\Delta^{(Q-1)} \\ z_{j\neq 1} &= \frac{1}{\Delta}\left(1 - \frac{\bar{z}_j}{\Delta^{N-Q}}\right) \quad . \end{aligned}$$

Then the BAE for $\bar{z}_j$ becomes

$$\begin{aligned} \bar{z}_1^N &= \frac{\left(\bar{z}_1 - \Delta^{-Q}\right)^{Q-1}}{\prod_{l\neq 1}^{Q}\bar{z}_j}, \\ \left(1 - \frac{\bar{z}_j}{\Delta^{N-Q}}\right)^N &= (-1)^{Q-1}\frac{\bar{z}_j^{Q-1}}{(\Delta^{-Q} - \bar{z}_1)\prod_{l\neq 1,j}\bar{z}_l} \quad . \end{aligned} \tag{43}$$

For macroscopic numbers of N and Q, the values of $\bar{z}_j/\Delta^{N-Q}$ and Δ^{-Q} are exponentially small and may be neglected. Thus the solution is

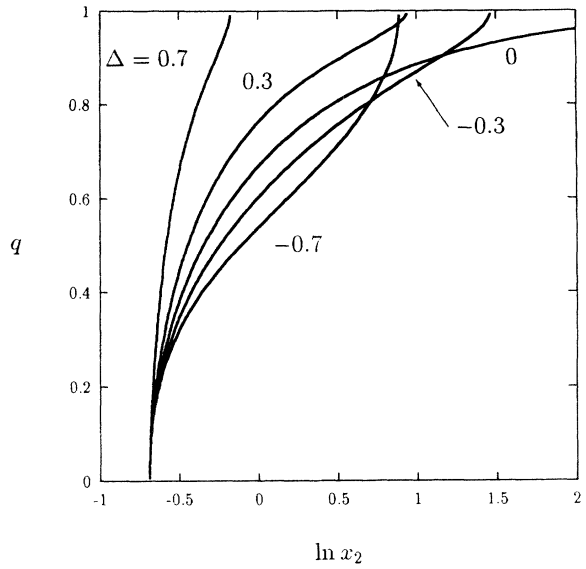

FIG. 6. Typical x_2 dependence of q within the IC phase is shown for $x_1 = x_2$. The curves are for $\Delta = -0.7, -0.3, 0, 0.3$, and 0.7, respectively.

$$\begin{aligned} \bar{z}_1 &= e^{i\theta}, \\ \bar{z}_{j\neq 1} &= \bar{z}_1 e^{i\pi(1+2j/Q)}, \end{aligned} \tag{44}$$

where θ can take the value from the set $\frac{2\pi}{N}\times\{1,\ldots,N\}$. The corresponding right eigenvector $|\lambda\rangle$ of the $\mathbf{T}_{R,Q} + \mathbf{T}_{L,Q}$ is

$$|\lambda\rangle = C\sum_{n_1<\cdots<n_Q} e^{in_1\theta}\Delta^{-\sum_{l=2}^{Q}(n_l-n_1)}|n_1,\ldots,n_Q\rangle, \tag{45}$$

where C is a normalizing constant. Here, $\{n_i\}$'s denote the position of up arrows or equivalently domain walls. It is obvious that these states represent bounded domain-wall states because the components of the eigenvector decay exponentially as the distance between domain walls becomes large. In fact, one can calculate the mean distance of the last domain wall from the first one. The mean distance $\langle n_Q - n_1\rangle$ of the Q domain-wall system is given by

$$\langle n_Q - n_1\rangle = \frac{\langle\lambda|\,(\hat{n}_Q - \hat{n}_1)\,|\lambda\rangle}{\langle\lambda|\lambda\rangle}, \tag{46}$$

where $\hat{n}_j$ is the position operator of the jth domain wall. Inserting the eigenket to the above expression and after some algebra, we find that $\langle n_Q - n_1\rangle$ is equal to Q for a macroscopic number of domain walls. Thus, we can interpret this state as the bounded domain-wall state.

This solution yields the exact configurational free energy which is obtained from the solution Eq. (44) with $\theta = 0$;

$$\kappa(q) = q\ln(\Delta+a) \quad . \tag{47}$$

And the free energy f for $\Delta > 1$ is simply

$$-\beta f = \max_{0\le q\le 1}\left[q\ln x_2 + q\ln(\Delta+a)\right] \quad . \tag{48}$$

The maximum value is obtained at $q = 0$ if x_2 is less than $1/(\Delta + a)$ and at $q = 1$ if x_2 is greater than $1/(\Delta + a)$. So there is a first-order phase transition between the two commensurate phases when x_2 is at the critical fugacity x_c, where

$$x_c = \frac{1}{\Delta + a} \qquad (\Delta > 1) \quad . \tag{49}$$

Note that the condition $w_1 = w_2$ used in [17] is amount to the condition $x_2 = 1/(\Delta + a)$ so that the first-order transition for $\Delta > 1$ could not to be seen in [17]. We have thus found the phase boundary of the C phase with domain-wall density $q = 0$ and 1 and the nature of the phase transition. We present the resulting phase diagram in Fig. 7(a) for the case of $a = 1$.

(iv) $\Delta < -4$, $q = 1/2^-$. As discussed before, we expect that f has a singularity in x_2 at $q = 1/2$ if Δ is large and negative. To see the q dependence of x_2 near $q = 1/2$, we should evaluate the configurational free energy $\kappa(q)$ near $q = 1/2$. Gulácsi, Beijeren, and Levi [17] used the root density function $\rho(p)$ to find the $q = 1/2$ phase boundary when $x_2(\Delta + a) = 1$. We employ the same method to the general case.

$\rho(p)$ is defined so as $N\rho(p)dp$ to be the number of the roots of the BAE [Eq. (17)] with $z = e^{ip}$ in the interval $(p, p + dp)$ in the complex p plane. We stress here that the roots do not lie on a straight line in the complex p plane. For domain-wall density q, $\rho(p)$ is given by [17]

$$\rho(p) = \frac{1}{2\pi}\left(1 + q\frac{\Delta e^{ip}}{1 - \Delta e^{ip}}\right) \quad . \tag{50}$$

In Fig. 8, we give a typical root distribution of the BAE in the complex α plane which is related to p as

$$e^{i\alpha} \equiv 1 - \Delta e^{ip} \quad . \tag{51}$$

The root density function $\tilde{\rho}(\alpha)$ in the α plane is given by

$$\tilde{\rho}(\alpha) \equiv \rho(p)\frac{dp}{d\alpha} = \frac{1}{2\pi}\left(-q + \frac{e^{i\alpha}}{e^{i\alpha} - 1}\right) \tag{52}$$

and the variables A, B and D in Fig. 8 are given by

$$q = \mathrm{Im}\left[\ln\left(e^{iA-B} - 1\right)\right]/(\pi + A),$$

$$\mathrm{Re}\left[\ln\frac{1 - e^{iA-B}}{\Delta}\right] + \frac{A}{\pi}\mathrm{Re}\left[\ln\left(e^{iA-B} - 1\right)\right]$$

$$+\frac{AB}{\pi} + \frac{1}{\pi}\sum_{n=1}^{\infty}\frac{e^{nB}}{n^2}\sin nA = 0, \tag{53}$$

$$D = 1 - \Delta C,$$

where C is determined from the equation

$$C = \frac{(1 - \Delta C)^q}{\exp\left[\frac{1}{N}\sum_{j=1}^{Q}\ln(1 - \Delta e^{ip_j})\right]} \quad . \tag{54}$$

Near $q = 1/2$, they take the values

$$A = \pi + (q - 1/2)\frac{1}{4\pi}\frac{1 - \lambda}{1 + \lambda} + O[(q - 1/2)^2],$$

$$B = \ln\lambda + O[(q - 1/2)^2], \tag{55}$$

$$D = 1 + \frac{|\Delta|}{2}\left(1 + \sqrt{1 + \frac{4}{|\Delta|}}\right)$$

$$+(q - 1/2)\ln(d\lambda)\Big/\left(\frac{1}{d-1} - \frac{1}{2d}\right) + O[(q - 1/2)^2],$$

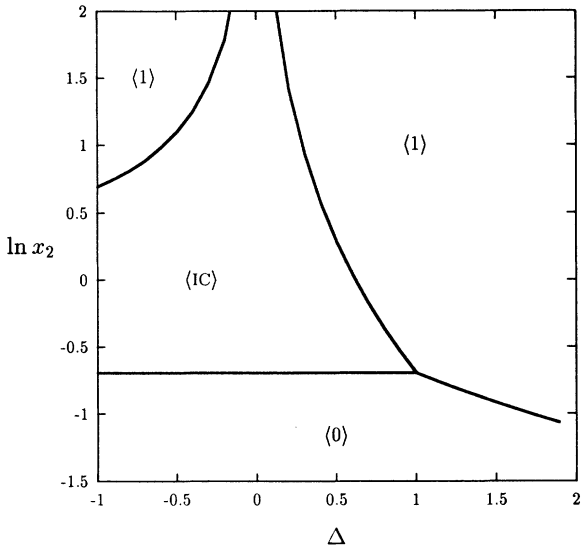

(a)

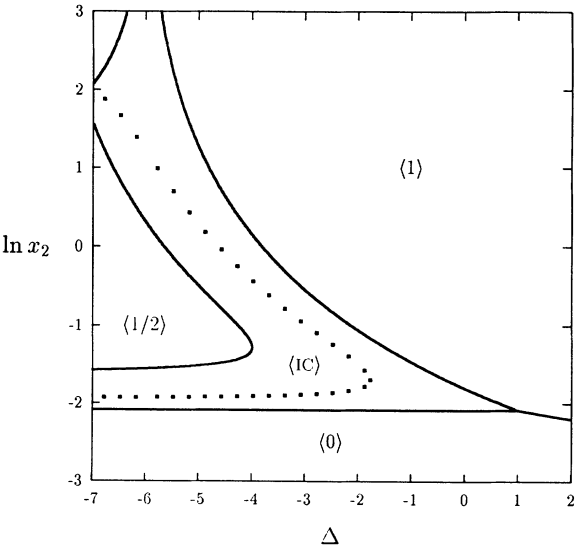

(b)

FIG. 7. (a) Phase diagram in the $\ln x_2$–Δ plane for $a = 1$. $\langle 0\rangle$, $\langle 1\rangle$, and $\langle \mathrm{IC}\rangle$ denote the C phase with $q = 0, 1$ and the IC phase, respectively. (b) Same as in (a) with $a = 7$. New C phase with $q = 1/2$ appears for $\Delta < -4$. The dotted line in the IC phase denotes the position where dislocations become irrelevant. See Sec. IV.

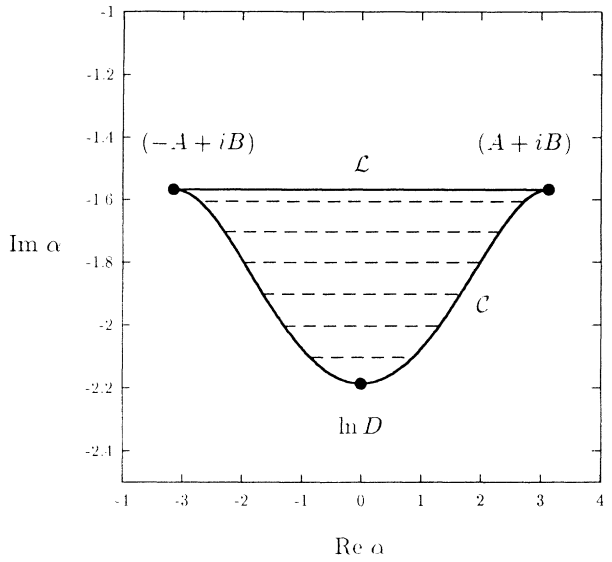

FIG. 8. A typical root distribution of the BAE in the complex α plane. This figure shows the solutions of BAE for $q = 1/2$ and $\Delta = -7$.

with

$$\lambda = \frac{1}{2}\left(|\Delta| - 2 - \sqrt{(|\Delta|-2)^2 - 4}\right) \quad . \tag{56}$$

With this knowledge, we can calculate $\kappa(q)$ near $q = 1/2$. First consider the case $q < 1/2$, where $\kappa(q)$ is evaluated from Eq. (20).

$$\begin{aligned}\kappa(q) &= \frac{1}{N}\sum_{j=1}^{Q} \ln\left(1 + ae^{ip_j}\right) \\ &= \int_C d\alpha\ \tilde{\rho}(\alpha)\ \ln\left(\frac{a + \Delta - ae^{i\alpha}}{\Delta}\right),\end{aligned} \tag{57}$$

where the integration should be taken along the contour C shown in Fig. 8. But, the contour can be deformed to the straight line $\mathcal{L}$ since the integrand is analytic in the shaded region. Then $\kappa(q)$, up to the first order in $(q - 1/2)$, is given by

$$\begin{aligned}\kappa(q) &= \frac{1}{2\pi}\int_{-A}^{A}\left[-q + \frac{e^{it}/\lambda}{e^{it}/\lambda - 1}\right]\ln\left(\frac{a + \Delta - ae^{it}/\lambda}{\Delta}\right) \\ &= \frac{1}{2}\ln a + (q - 1/2)\left[\ln\frac{a}{|\Delta|\lambda} + 2\ln\left(1 + \frac{a+\Delta}{a}\lambda\right)\right] \\ &\quad + O[(q-1/2)^2] \quad .\end{aligned} \tag{58}$$

Note that $\kappa(1/2) = \frac{1}{2}\ln a$ is independent of Δ. This implies that there are only type-1 domain walls without adjacent pairs of them at the $q = 1/2$ phase. From Eq. (31), we see that $q = 1/2$ phase starts at $x_2 = x_-$ where

$$\ln x_- = -\ln\frac{a}{|\Delta|\lambda} - 2\ln\left[1 + \frac{a+\Delta}{a}\lambda\right] \quad . \tag{59}$$

(v) $\Delta < -4$, $q = 1/2^+$. Next consider the case $q > 1/2$, where the configurational free energy is evaluated from Eq. (21). For convenience, we define two quantities $\mathcal{A}$ and $\mathcal{B}$;

$$\begin{aligned}\mathcal{A} &\equiv \frac{1}{N}\sum^{\bar{Q}} \ln\left(1 - \Delta e^{ip_j}\right) \\ \mathcal{B} &\equiv \frac{1}{N}\sum^{\bar{Q}} \ln\left[1 - (a+\Delta)e^{ip_j}\right].\end{aligned} \tag{60}$$

Then the configurational free energy is written as

$$\kappa(q) = \max\{\kappa_L(q),\ \kappa_R(q)\}, \tag{61}$$

where $\kappa_L = \mathcal{A} - \mathcal{B}$ and $\kappa_R = \ln a + q\ln[(a+\Delta)/a] - \mathcal{B}$. The quantities $\mathcal{A}$ and $\mathcal{B}$ can be written as contour integrations in the complex α plane in the thermodynamic limit $N \to \infty$.

$$\begin{aligned}\mathcal{A} &= \int_C d\alpha\ i\alpha\ \tilde{\rho}(\alpha) \\ \mathcal{B} &= \int_C d\alpha\ \tilde{\rho}(\alpha)\ \ln\left(\frac{a - (a+\Delta)e^{i\alpha}}{|\Delta|}\right).\end{aligned} \tag{62}$$

Since the integrand in $\mathcal{A}$ is analytic in the shaded region, the contour can be deformed to the straight line $\mathcal{L}$ and the integration results in

$$\mathcal{A} = \frac{1}{2}\ln|\Delta| - (\bar{q} - \tfrac{1}{2})\ln\lambda + O[(\bar{q} - 1/2)^2] \quad . \tag{63}$$

In order to calculate $\mathcal{B}$, there are three possible cases to consider;

(a) $1/D < \lambda < (a+\Delta)/a$. The integrand is also analytic in the shaded region and the contour C is replaced by the straight line $\mathcal{L}$. It yields

$$\begin{aligned}\mathcal{B}_a &= \frac{1}{2}\ln(a+\Delta) \\ &\quad + (\bar{q} - 1/2)\left[\ln\frac{a+\Delta}{|\Delta|\lambda} + 2\ln\left(1 + \frac{a\lambda}{a+\Delta}\right)\right] \\ &\quad + O\left[(\bar{q} - 1/2)^2\right] \quad .\end{aligned} \tag{64}$$

(b) $1/D < (a+\Delta)/a < \lambda$. In this case, the branch cut intrudes into the shaded area. Therefore, upon changing C to the straight line, one needs to subtract the contribution around the branch cut. The result is

$$\begin{aligned}\mathcal{B}_b &= \frac{1}{2}\ln(a+\Delta) \\ &\quad + (\bar{q} - 1/2)\left[\ln\frac{a+\Delta}{|\Delta|\lambda} + 2\ln\left(1 + \frac{a\lambda}{a+\Delta}\right)\right] \\ &\quad + O\left[(\bar{q} - 1/2)^2\right] \quad .\end{aligned} \tag{65}$$

(c) $(a+\Delta)/a < 1/D < \lambda$. In this case, the contour can be deformed to the straight line $\mathcal{L}$ as in the case (a) and the integration results in

$$\begin{aligned}\mathcal{B}_c &= \frac{1}{2}\ln\frac{|\Delta|}{a} + (\bar{q} - 1/2)\left[\ln\frac{a}{|\Delta|} + 2\ln\left(1 + \frac{a+\Delta}{a\lambda}\right)\right] \\ &\quad + O\left[(\bar{q} - 1/2)^2\right] \quad .\end{aligned} \tag{66}$$

For each case, the quantity κ_R and κ_L take the following values at $q = 1/2$:

$$\begin{aligned}
&\text{(a)}\ \kappa_L = \tfrac{1}{2}\ln\tfrac{|\Delta|}{a+\Delta}\ ,\ \kappa_R = \tfrac{1}{2}\ln a \\
&\text{(b)}\ \kappa_L = \tfrac{1}{2}\ln\tfrac{|\Delta|}{a+\Delta}\ ,\ \kappa_R = \tfrac{1}{2}\ln a \\
&\text{(c)}\ \kappa_L = \tfrac{1}{2}\ln a\ \ ,\ \kappa_R = \tfrac{1}{2}\ln a + \tfrac{1}{2}\ln\tfrac{a(a+\Delta)}{|\Delta|}\ .
\end{aligned} \tag{67}$$

When $a+\Delta > 1$, only the cases (a) and (b) in Eq. (67) occur and $\kappa_R > \kappa_L$ at $q = 1/2$. So near $q = 1/2$, the configurational free energy $\kappa(q)$ is determined by $\kappa_R(q)$ and is given by

$$\kappa(q) = \frac{1}{2}\ln a + (q-1/2)\left[\ln\frac{\lambda a}{|\Delta|} + 2\ln\left(1+\frac{a+\Delta}{a\lambda}\right)\right] + O[(q-1/2)^2]. \tag{68}$$

When $a+\Delta < 1$, cases (b) and (c) occur. One can easily find that if $(a+\Delta)/a < 1/D$ then $\kappa_L > \kappa_R$ and if $(a+\Delta)/a > 1/D$ then $\kappa_L < \kappa_R$. So, near $q = 1/2$ the configurational free energy is

$$\begin{aligned}
\kappa(q) &= \begin{cases} \kappa_L(q) & \text{if } (a+\Delta)/a < 1/D \\ \kappa_R(q) & \text{if } (a+\Delta)/a > 1/D \end{cases} \\
&= \frac{1}{2}\ln a + (q-1/2)\left[\ln\frac{\lambda a}{|\Delta|} + 2\ln\left(1+\frac{a+\Delta}{a\lambda}\right)\right] \\
&\quad + O[(q-1/2)^2].
\end{aligned} \tag{69}$$

From Eqs. (68) and (69), we see that the $q = 1/2$ phase ends at $x_2 = x_+$ where

$$\ln x_+ = -\ln\frac{a\lambda}{|\Delta|} - 2\ln\left(1+\frac{a+\Delta}{a\lambda}\right). \tag{70}$$

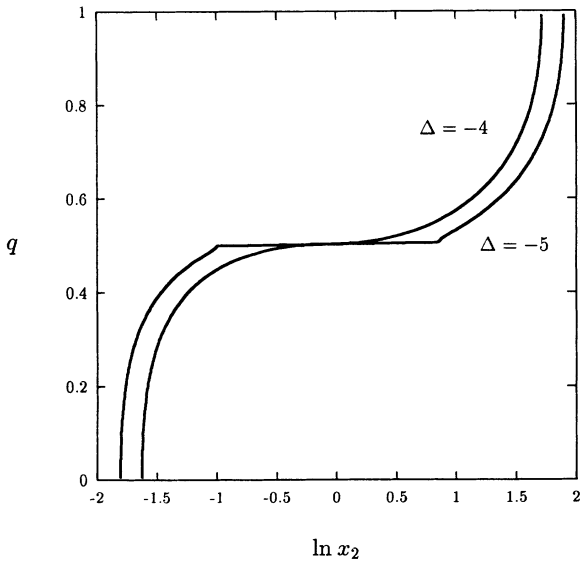

FIG. 9. Typical x_2 dependence of the domain-wall densities for $\Delta = -4.0$ and -5.0. The curves are for $a = \Delta + 0.1$. This is obtained from the equation of state [Eq. (31)] where configurational free energy is taken from the numerical solution of the BAE with $N = 150$.

x_- [Eq. (59)] and x_+ [Eq. (70)] defines the phase boundary between the $q = 1/2$ C phase and the IC phase and the domain-wall density is locked at $q = 1/2$ for the range

$$x_- < x_2 < x_+ \ . \tag{71}$$

Since x_- and x_+ merge at $\Delta_c = -4$, this phase appears only when $a > 4$. Figure 7(b) shows the full phase boundaries for $a = 7$ and Fig. 9 shows the domain-wall density as a function of $\ln x_2$ for $\Delta = -4$ and -5.

IV. THE CRITICAL PROPERTIES OF THE IC PHASE

The conformal-field theory predicts that the operator content of a critical phase is related to the finite-size correction to the eigenvalue spectra of the transfer matrix [21]. When we write an eigenvalue Λ_α of the transfer matrix for a lattice of width N as e^{-E_α}, then E_α takes the form at the criticality,

$$E_\alpha = Nf_\infty + \frac{2\pi}{N}\left(\Delta_\alpha + \bar{\Delta}_\alpha - \frac{c}{12}\right)\zeta\sin\theta + \frac{2\pi i}{N}\left(\Delta_\alpha - \bar{\Delta}_\alpha\right)\zeta\cos\theta + o\left(\frac{1}{N}\right)\ , \tag{72}$$

where c is the central charge, $(\Delta_\alpha, \bar{\Delta}_\alpha)$ are the conformal dimensions of the operator corresponding to the αth energy eigenstate, ζ is the anisotropy factor, θ is the anisotropy angle, and finally f_∞ is the nonuniversal bulk free energy per site in units of kT [21,22].

The *toroidal partition function* (TPF) $\tilde{\mathcal{Z}}$ is defined as the order 1 part of the partition function $\mathcal{Z}$ for conformally invariant system of N columns and M rows. It follows from Eq. (72) that

$$\begin{aligned}
\tilde{\mathcal{Z}} &\equiv \lim_{\substack{N,M\to\infty \\ M/N=\text{fixed}}} \sum_\alpha e^{-ME_\alpha}/e^{-NMf_\infty} \\
&= \sum_\alpha \exp\left[-\frac{2\pi M\zeta}{N}\left\{\left(\Delta_\alpha + \bar{\Delta}_\alpha - \frac{c}{12}\right)\sin\theta + i\left(\Delta_\alpha - \bar{\Delta}_\alpha\right)\cos\theta\right\}\right] \\
&= (q\bar{q})^{-c/24}\sum_\alpha q^{\Delta_\alpha}\bar{q}^{\bar{\Delta}_\alpha},
\end{aligned} \tag{73}$$

where q, the modular parameter, is given by

$$q = e^{2\pi i\tau} \tag{74}$$

with

$$\tau = \frac{M}{N}\zeta e^{i(\pi-\theta)}\ , \tag{75}$$

$\bar{q}$ is the complex conjugate of q and the sum is over the infinite set of levels whose energy E_α scales as Eq. (72). In the first part of this section we use the notation q to denote the modular parameter [Eq. (74)]. This is not to be confused with the domain-wall density.

For the Gaussian model compactified on a circle, or equivalently, the symmetric six-vertex model in the continuum limit, the TPF under periodic boundary conditions in both directions is given by the $c = 1$ Coulombic partition function [23]

$$\widetilde{\mathcal{Z}}_C(g) = \frac{1}{|\eta(q)|^2} \sum_{n,m\in\mathbf{Z}} q^{\Delta_{n,m}(g)} \bar{q}^{\Delta_{n,-m}(g)}, \tag{76}$$

where g is the so-called Gaussian coupling constant, $\Delta_{n,m} = \frac{1}{4}\left(\frac{n}{\sqrt{g}} + \sqrt{g}m\right)^2$ and $\eta(q)$ is the Dedekind eta function;

$$\eta(q) = q^{\frac{1}{24}} \prod_{n=1}^{\infty}(1-q^n) \quad . \tag{77}$$

One can impose $U(1)$ boundary conditions on the six-vertex model instead of periodic boundary conditions. In the Pauli spin representation, the twisted boundary condition is

$$\left(\sigma^x_{N+1} \pm i\sigma^y_{N+1}\right) = e^{\mp i\varphi}\left(\sigma^x_1 \pm i\sigma^y_1\right), \tag{78}$$

where φ is the twisting angle. The Coulombic toroidal partition function is then modified to [24]

$$\widetilde{\mathcal{Z}}_C(g) = \frac{1}{|\eta(q)|^2} \sum_{n,m\in\mathbf{Z}} e^{-in\varphi'} q^{\Delta_{n,m-\varphi/2\pi}(g)} \bar{q}^{\Delta_{n,-(m-\varphi/2\pi)}(g)}, \tag{79}$$

where φ and φ' are the twisting angles in the space and time directions, respectively.

After this short review, we now turn to the critical properties of the IC phase. It is generally known that the striped IC phase is critical and described by the $c = 1$ conformal-field theory in the continuum limit [1,25]. In the fermion model approach, Park and Widom [6] calculated exact toroidal partition function explicitly for the free fermion, i.e., noninteracting domain-wall system and showed that it is of the form of Eq. (79) where $g = 1/2$, $\varphi' = 0$, and $\varphi/2\pi$ is the number of the domain walls per row (mod 1). Note that the twisted boundary condition used in Ref. [6] has no direct physical meaning.

For the $T = 0$ TAFIM without the second-neighbor interaction, the central charge and the scaling dimensions of several operators are calculated analytically [25]. Since all the transfer matrix spectra are known from the Onsager solution in this case, one may go one step further and calculate the toroidal partition function explicitly. We present the calculation in Appendix B.

When $\Delta = 0$, the TPF $\widetilde{\mathcal{Z}}_{5\text{-}v}$, of the five-vertex model can be obtained from the $\widetilde{\mathcal{Z}}^{(\mu,\nu)}_{\text{TAFIM}}$ of Appendix B, by using the relation Eq. (15). The result is

$$\begin{aligned}\widetilde{\mathcal{Z}}_{5\text{-}v} &= \frac{|\tilde{q}|^{\alpha^2}}{2|\eta(\tilde{q})|^2}\left\{|\vartheta_1(z,\tilde{q})|^2 + |\vartheta_2(z,\tilde{q})|^2 + |\vartheta_3(z,\tilde{q})|^2 + |\vartheta_4(z,\tilde{q})|^2\right\} \\ &= \frac{1}{|\eta(\tilde{q})|^2} \sum_{n,m\in\mathbf{Z}} e^{-2i\alpha_0 Mm} \tilde{q}^{(m+\frac{n+2\alpha}{2})^2/2} \bar{\tilde{q}}^{(m-\frac{n+2\alpha}{2})^2/2} \quad (\Delta = 0)\ .\end{aligned} \tag{80}$$

This takes the final form after the modular transformation $\tilde{\tau} \to \tau = -1/\tilde{\tau}$;

$$\widetilde{\mathcal{Z}}_{5\text{-}v} = \frac{1}{|\eta(q)|^2} \sum_{m,n\in\mathbf{Z}} e^{-i\pi Q_1 m} q^{\Delta_{m,n-Q_0}(g=1/2)} \bar{q}^{\Delta_{m,-(n-Q_0)}(g=1/2)} \quad (\Delta = 0), \tag{81}$$

where Q_0 and Q_1 are given in Eqs. (B28) and (B29), respectively. This is the exactly Coulombic partition function with the twisting angle $\varphi = 2\pi Q_0$ and $\varphi' = \pi Q_1$.

Note that this can be also obtained by replacing (m,n) in Eq. (B30) by $(2m, n/2)$. In Sec. II, we gave the relation between the transfer matrices of the $T = 0$ TAFIM and the five-vertex model. $\mathbf{T}_{5\text{-}v}$ contains odd Q sectors while $\mathbf{T}^{(0)}_{\text{TAFIM}}$ contains the spin-reversal odd sector, $\mathbf{T}_L - \mathbf{T}_R$. So, one expects $\widetilde{\mathcal{Z}}_{5\text{-}v}$ can be obtained from $\widetilde{\mathcal{Z}}^{(0,0)}_{\text{TAFIM}}$ by adding terms coming from the odd Q sectors and eliminating the terms originated from $\mathbf{T}_L - \mathbf{T}_R$. Our results show that this is exactly done by a simple substitution of (m,n) by $(2m, n/2)$.

Equation (81) implies that the IC phase of the noninteracting domain-wall model is in the universality class of the Gaussian model with coupling constant $g = 1/2$ regardless of the anisotropies in the fugacity of the domain walls. This result is in accord with previous works but it confirms the universality in the strongest sense.

We assume that the effect of domain-wall interactions preserves the $c = 1$ nature throughout the IC phase even though it may change the modular parameters, the coupling constant, etc. Since the coupling constant g determines the critical exponents, its possible dependence on interactions over the IC phase is of interest. If we denote the eigenvalue of $\mathbf{T}_{5\text{-}v}$ corresponding to the mth spin-wave operator in the sector Q by $e^{-E_{m,Q}}$, it is expected to take the form in the IC phase

$$\begin{aligned}\mathrm{Re}\{E_{m,Q}\} = \frac{2\pi\zeta\sin\theta}{N}\left(\frac{g}{2}(Q-Q_0)^2 + \frac{m^2}{2g} - \frac{c}{12}\right) \\ + Nf_\infty,\end{aligned} \tag{82}$$

where $Q_0 = qN$ is the average number of domain walls per row. Here and below, q denotes the domain-wall density. We now calculate g perturbatively in the small Δ limit and numerically for a wide range of Δ. During the perturbative calculation with $|\Delta| < 1$, we will only consider the isotropic case ($a = 1$) for simplicity. In this case, the eigenvalue $e^{-E_{m,Q}}$ of the transfer matrix with $\Delta = 0$ is

$$\mathrm{Re}\{E_{m,Q}(\Delta = 0)\} = \frac{2\pi\zeta^0}{N}\left(\frac{m^2}{2g^0} + \frac{g^0(Q-Q_0)^2}{2} - \frac{c}{12}\right) + Nf_\infty, \tag{83}$$

where $c = 1$, $\zeta^0 = \frac{1}{2}\tan(\pi q/2)$, and $g^0 = \frac{1}{2}$ as given in Appendix B and the superscripts in g^0 and ζ^0 denote the value for the noninteracting case. If we insert $p_j = n_j + u_j$ into the BAE where $n_j = I_j + m$ is the solution of the $\Delta = 0$ BAE for the mth excited state in a given Q sector, the resulting equation for u_j is, up to the first order in Δ,

$$u_j = iq\left[s + \Delta e^{-qs}e^{in_j}\right], \tag{84}$$

where s is

$$s = -\Delta\frac{\sin\pi q}{\pi q}e^{2\pi im/N}\left(1 + \frac{\pi^2}{6N^2}\right) \tag{85}$$

that is determined from the condition $\sum_j u_j = 0$. With this solution $\{u_j\}$, we can calculate the energy shift $\delta E_{m,Q} \equiv E_{m,Q}(\Delta \neq 0) - E_{m,Q}(\Delta = 0)$ due to the interaction

$$\frac{1}{N}\mathrm{Re}\{\delta E_{m,Q}\} = -\sum_j \ln\frac{1+e^{i(n_j+u_j)}}{1+e^{in_j}} = \frac{q}{N}\sum_j \frac{se^{in_j} + \Delta e^{2in_j}}{1+e^{in_j}}$$
$$= \Delta\left(\frac{q^2}{2} + \frac{q}{2\pi}\sin\pi q\right) + \Delta\left(2\sin^2\frac{\pi q}{2} - \pi q\sin\pi q\right)\left(\frac{m}{N}\right)^2 + \Delta\frac{\pi}{6N^2}\left(\frac{q}{2}\sin\pi q\right) + O\left(\frac{1}{\Delta^2}\right) . \tag{86}$$

Using the value of $\mathrm{Re}\{E_{m,Q}\}/N$ at $\Delta = 0$, we can write down the energy $\mathrm{Re}\{E_{m,Q}(\Delta)\}$ up to the first order in Δ.

$$\frac{1}{N}\mathrm{Re}\{E_{m,Q}(\Delta)\} = \frac{1}{N}\mathrm{Re}\{E_{m,Q}(\Delta = 0)\} + \frac{1}{N}\mathrm{Re}\{\delta E_{m,Q}\}$$
$$= f'_\infty + 2\pi\left(\frac{Q-Q_0}{N}\right)^2\left[\frac{\zeta^0 g^0}{2} - \frac{\Delta}{8\pi}\left(\pi q\sin\pi q + 4\sin^2\frac{\pi q}{2}\right)\right]$$
$$+2\pi\left(\frac{m}{N}\right)^2\left[\frac{\zeta^0}{2g^0} + \frac{\Delta}{2\pi}\left(2\sin^2\frac{\pi q}{2} - \pi q\sin\pi q\right)\right] - \frac{\pi}{6N^2}\left(\zeta^0 c^0 - \frac{\Delta q}{2}\sin\pi q\right) + O\left(\frac{1}{\Delta^2}\right)$$
$$\equiv f'_\infty + \frac{2\pi\zeta}{N^2}\left(\frac{g}{2}(Q-Q_0)^2 + \frac{1}{2g}m^2 - c/12\right) . \tag{87}$$

The new anisotropy factor ζ, the Gaussian coupling constant g and the central charge c are obtained by comparing the last two expressions,

$$\begin{aligned} c &= 1, \\ g &= \tfrac{1}{2}\left(1 - \tfrac{2\Delta}{\pi}\sin\pi q\right) + O(\Delta^2), \\ \zeta &= \tfrac{1}{2}\tan\tfrac{\pi q}{2}\left(1 - 2\Delta q\cos^2\tfrac{\pi q}{2}\right) + O(\Delta^2) . \end{aligned} \tag{88}$$

The result from the first-order perturbation calculation shows that the interaction between domain walls causes a continuous variation of the coupling constant g so the scaling dimensions vary continuously as a function of the interaction parameter Δ.

For larger values of Δ, g can be evaluated numerically by the finite-size corrections of the eigenvalue of the transfer matrix [Eq. (72)]. Suppose the model parameters are tuned in such a way that $Q_0 = Nq$ is an integer. That is, we are considering the case of q being integer multiple of $1/N$. From Eq. (82), g and $\zeta\sin\theta$ can be evaluated if we calculate four eigenvalues $E_{m,Q}$ with $(m,Q) = (0,Q_0), (0,Q_0\pm1)$ and $(1,Q_0)$.

$$g = \sqrt{\mathrm{Re}\{E_{0,Q_0+1} + E_{0,Q_0-1} - 2E_{0,Q_0}\}/\mathrm{Re}\{E_{1,Q_0} - E_{0,Q_0}\}/2}$$
$$\zeta\sin\theta = \frac{N}{\pi}\sqrt{\mathrm{Re}\{E_{0,Q_0+1} + E_{0,Q_0-1} - 2E_{0,Q_0}\}\mathrm{Re}\{E_{1,Q_0} - E_{0,Q_0}\}/2} . \tag{89}$$

Necessary $E_{m,Q}$'s are obtained by solving the BAE for N up to 150. The coupling constant g obtained in this way is shown in Fig. 10 as a function of q for several values of Δ for a particular value of $a = |\Delta| + 0.1$. Note that the value of g starts from around $1/2$ at $q = 0$ and ends at $1/2$ at $q = 1$ and varies smoothly when $\Delta > -4$. The values $g = 1/2$ at $q = 0$ are easily understood since the interaction effect will vanish in these limits. So is

the case for $q = 1$ and $\Delta + a < 1$. When $\Delta \leq -4$, the value of g approaches 2 as $q \to 1/2$. The fact that $g = 2$ exactly in the $q \to 1/2$ limit can be derived analytically following the procedure similar to that used by Gwa and Spohn [26].

The domain-wall model is obtained from the TAFIM by neglecting the spin configurations in which three spins on any elementary triangle are in the same state. This excitation driven by the thermal fluctuation creates or annihilates two domain walls at a time and causes a domain-wall density dislocation. (See Fig. 11.) When two dislocations of up triangle and down triangle occur in pair, the density dislocation remains as a local defect. These pair excitations are analogous to the vortex and antivortex pair excitations in the XY model. The scaling dimension for the density dislocation [9] is $x_{0,2} \equiv \Delta_{0,2} + \Delta_{0,-2}$ since such excitation creates or annihilates two domain walls. Since $x_{0,2} = 2g$ we see that when $g < 1$ ($x_{0,2} < 2$) the density dislocation is relevant and destroys the criticality of the IC phase. Therefore, if dislocations are allowed with finite costs of energy, the IC phase cannot remain critical and becomes the disordered fluid phase. On the other hand, when $g > 1$ ($x_{0,2} > 2$) the density dislocation is irrelevant and the criticality of the IC phase survives. At the boundary $g = 1$, the Kosterlitz-Thouless (KT) transition would occur. Since the noninteracting domain-wall system has $g = 1/2$, the critical IC phase cannot survive from the density dislocation. However as seen in Fig. 10, g crosses the critical value $g = 1$ in the region of repulsive ($\Delta < 0$) interactions. The dotted line in Fig. 7(b) inside the IC phase denotes the position where g takes the value 1.

So, we conclude that the IC phase near the $q = 1/2$ C phase is stable under the density dislocation. This shows that there are three phases encountered if we consider the dislocation effect. They are long-range ordered $q = 1/2$ C phase, quasi-long-range ordered IC phase, and the disordered phase. They are separated by the PT transition and the KT transition. It also explains the phase diagram of the TAFIM with the isotropic NNN interaction obtained by Monte Carlo simulation [11].

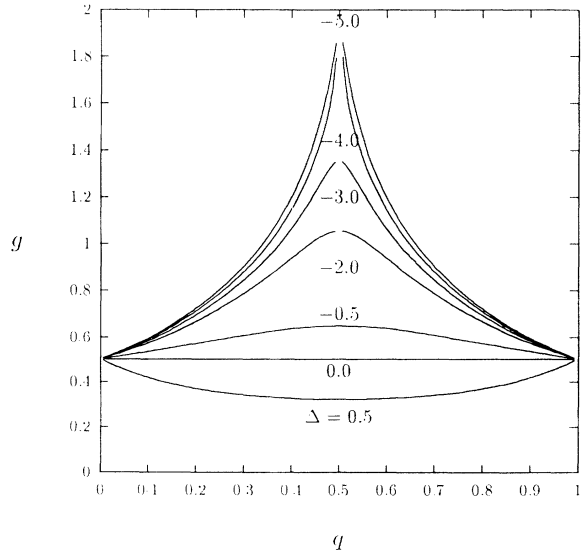

FIG. 10. The Gaussian coupling constant g calculated numerically with lattice size $N = 150$ and $\Delta = 0.5, 0.0, -0.5, -2.0, -3.0, -4.0$, and -5.0. For each curve, a is set to the value $a = |\Delta| + 0.1$.

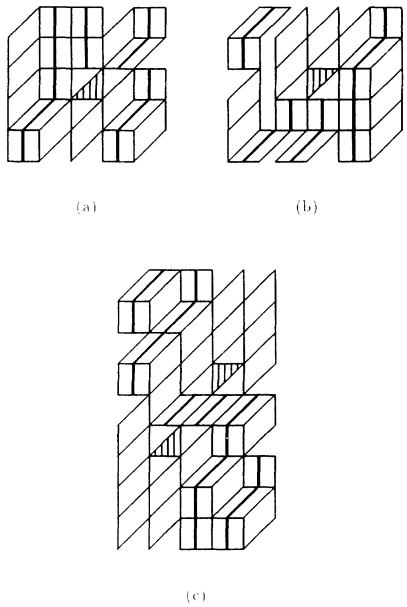

FIG. 11. Effect of finite temperature in TAFIM is to excite dislocations in domain walls. Simultaneous creation of vortex (a) and antivortex (b) pairs as in (c) destroys the IC phase if $g < 1$ but is irrelevant if $g > 1$.

V. SUMMARY AND DISCUSSION

In this work, we have introduced a solvable interacting-domain-wall model derived from the $T = 0$ TAFIM with anisotropic nearest-neighbor and NNN interactions. The model is shown to be equivalent to the five-vertex model and exact phase diagram is obtained in the three-dimensional parameter space. It shows C phases where the domain-wall density is 0, 1/2, or 1 and the IC phase in between.

The IC phase is a critical phase described by the Gaussian fixed point. The Gaussian coupling constant g which determines the scaling dimensions of operators is a function of the model parameters and changes smoothly from 1/2 at $q = 0$ and $q = 1$ phase boundaries to 2 at the $q = 1/2$ phase boundary. As the interaction is turned on, it decreases (increases) for the attractive (repulsive) interaction. For strong repulsive interactions, there is a region with $g > 1$ in which dislocation is irrelevant. Therefore the scenario proposed by Nienhuis, Hilhorst, and Blöte for the effect of the isotropic NNN interaction in the $T = 0$ TAFIM is partly born out in this model.

We also have shown by the explicit calculation of the TPF of the noninteracting T=0 TAFIM that it renormalizes to the Gaussian fixed point with the coupling constant g=2. This is in accord with previous works. But, the transfer matrix spectra of the five-vertex model with $\Delta = 0$ and that of the noninteracting T=0 TAFIM

are different in that some sectors present in one are absent in the other. This redistribution of sectors or operator content changes g of the five-vertex model to $1/2$ when $\Delta = 0$. The TPF of the five-vertex model is found to take the form of the symmetric six-vertex model with the twisted boundary conditions. A fractional part of the number of domain walls across a row and a column determines the twisting angles of $U(1)$ boundary conditions along the space and time directions, respectively.

The model considered in this work is rather special in that only one type of domain wall interacts. For the fully interacting case, say $y_1 = y_2 = y$, one needs to rely on less accurate numerical methods. The effects of the interaction between domain walls in both directions on the phase diagram and the critical properties of the IC phase are of interest and left for further works.

ACKNOWLEDGMENTS

We thank discussions with F. Y. Wu and H. Park. This work was supported by KOSEF through the grant to Center for Theoretical Physics. J. D. Noh also thanks the Dawoo Foundation for its support.

APPENDIX A

In this appendix, we discuss the Yang-Baxter equation (YBE) of the five-vertex model and alternative parametrization from which the corresponding quantum chain Hamiltonian is derived.

The YBE for the five-vertex model is given by

$$(\mathbf{1}\otimes\mathbf{R})\,(\mathbf{R}'\otimes\mathbf{1})\,(\mathbf{1}\otimes\mathbf{R}'') = (\mathbf{R}''\otimes\mathbf{1})\,(\mathbf{1}\otimes\mathbf{R}')\,(\mathbf{R}\otimes\mathbf{1}), \quad \text{(A1)}$$

where $\mathbf{1}$ is the 2×2 unit matrix, $\otimes$ denotes the direct product, $\mathbf{R}$ is the 4×4 matrix given by

$$\mathbf{R} = \begin{pmatrix} w_1 & 0 & 0 & 0 \\ 0 & w_5 & w_3 & 0 \\ 0 & w_4 & w_6 & 0 \\ 0 & 0 & 0 & w_2 \end{pmatrix}, \quad \text{(A2)}$$

and finally $\mathbf{R}'$ ($\mathbf{R}''$) is the same as $\mathbf{R}$ with w_i replaced by w_i' (w_i''). When $w_3 = w_3' = 0$, the YBE has a solution provided

$$\Delta = \frac{w_1w_2 - w_5w_6}{w_2w_4} = \frac{w_1'w_2' - w_5'w_6'}{w_2'w_4'}. \quad \text{(A3)}$$

The solution under the normalization $w_2 = w_2' = w_2'' = 1$ is

$$\begin{aligned} w_1'' &= w_1'/w_1, \\ w_3'' &= 0, \\ w_4'' &= (w_1w_4' - w_4w_1')/(w_5w_6), \\ w_5'' &= w_5'/w_5, \\ w_6'' &= w_6'/w_6. \end{aligned} \quad \text{(A4)}$$

As a result, the transfer matrix of $\mathbf{T}_{5\text{-}v}$ having three independent parameters forms a two-parameter family of commuting matrices. Vertex weights of the five-vertex model used in this work is given by Eq. (6). If one parametrizes them alternatively as

$$\begin{aligned} w_1 &= e^v, \\ w_2 &= 1, \\ w_3 &= 0, \\ w_4 &= (e^v - e^u)/\Delta, \\ w_5 &= w_6 = e^{u/2}, \end{aligned} \quad \text{(A5)}$$

and similarly for w_i''s, the transfer matrices $\mathbf{T}_{5\text{-}v}(u,v;\Delta)$ with different u and v commute, i.e.,

$$[\,\mathbf{T}_{5\text{-}v}(u,v;\Delta)\;,\;\mathbf{T}_{5\text{-}v}(u',v';\Delta)\,] = 0 \quad \text{(A6)}$$

for all u, u',v, and v'. Equation (A4) with above parametrization becomes

$$\begin{aligned} w_1'' &= e^{v'-v}, \\ w_4'' &= e^v(e^{v'-v} - e^{u'-u})/\Delta, \\ w_5'' &= w_6'' = e^{(u'-u)/2}. \end{aligned} \quad \text{(A7)}$$

Standard parametrizations of solutions to the YBE involve the so-called spectral parameter u with which the YBE displays the difference property; i.e., if $\mathbf{R} = \mathbf{R}(u)$ and $\mathbf{R}' = \mathbf{R}(u')$ then $\mathbf{R}'' = \mathbf{R}(u'-u)$. At criticality, it gives the physical meaning of the anisotropy angle [22]. Also, the corresponding quantum chain Hamiltonian commuting with the transfer matrix is obtained by the logarithmic derivative at $u = 0$. We find from Eq. (A7) that the five-vertex model also displays the difference property if we set $v = 0$. This is the special case $w_1 = w_2$ considered in Ref. [17].

We calculated the quantum Hamiltonian $\hat{\mathcal{H}}$ of the one-dimensional quantum spin chain by taking the logarithmic derivative of the transfer matrix at $u = 0$ for the case of $v = 0$. The result is

$$\begin{aligned} \hat{\mathcal{H}} &= \mathbf{T}_{5\text{-}v}^{-1}\left.\frac{\partial \mathbf{T}_{5\text{-}v}}{\partial u}\right|_{u,v=0} \\ &= \sum_{i=1}^{N}\left\{\hat{s}_i^+\,\hat{s}_{i+1}^- + \frac{\Delta}{4}\,\hat{s}_i^z\,\hat{s}_{i+1}^z\right\}, \end{aligned} \quad \text{(A8)}$$

where $\hat{s}_i$ is the quantum spin density operator at site i. This non-Hermitian Hamiltonian is similar to the Hamiltonian of the XXZ quantum spin chain. The difference is that there is no term $\hat{s}_i^-\,\hat{s}_{i+1}^+$ in this model. So, there is a net flux of the spin flow from the right to the left of the chain. It comes from the anisotropic choice of the vertex weights at the beginning.

APPENDIX B

In this appendix, we present the phase diagram of the $T = 0$ TAFIM with anisotropic nearest-neighbor interaction and the toroidal partition functions under the general boundary conditions.

Through the star-triangle relation, the Ising model on the triangular lattice can be mapped into the Ising model on the honeycomb lattice [18]. Let $K_i = K + \delta_i$ and

L_i $(i = 1,2,3)$ be the interaction strength (including the factor $-1/kT$) of the Ising model on the triangular and honeycomb lattice, respectively. Then, the partition functions $\mathcal{Z}_{\rm TAFIM}$ on a triangular lattice with $\mathcal{N}$ sites and $\mathcal{Z}_{\rm H}$ on a honeycomb lattice with $2\mathcal{N}$ sites are related by

$$\mathcal{Z}_{\rm H}(\boldsymbol{L}, 2\mathcal{N}) = R^{\mathcal{N}} \mathcal{Z}_{\rm TAFIM}(\boldsymbol{K}, \mathcal{N}) \tag{B1}$$

provided $\boldsymbol{K}$ and $\boldsymbol{L}$ satisfy the star-triangle relation:

$$\exp\left[K_1 s_2 s_3 + K_2 s_3 s_1 + K_3 s_1 s_2\right] = R \sum_{t=\pm 1} \exp\left[t(L_1 s_2 + L_2 s_2 + L_3 s_3)\right] \quad . \tag{B2}$$

Here R is the normalization factor.

If we take the zero-temperature limit $K \to -\infty$, the solution of the star-triangle relation is

$$\sinh 2L_i = \frac{z_i}{k} \ , \quad \cosh 2L_i = \frac{z_j^2 + z_k^2 - z_i^2}{2 z_j z_k} \ ,$$
$$R^2 = \frac{2 z_1 z_2 z_3}{k^2} \tag{B3}$$

where

$$z_i = e^{2\delta_i} \quad ,$$
$$k^2 = (4 z_i^2 z_j^2 z_k^2)/[(z_j^2 + z_k^2 - z_i^2)^2 - 4 z_j^2 z_k^2]$$

and (i,j,k) is a cyclic permutation of (1,2,3).

Now, we consider the transfer matrix $\mathbf{T}_{\rm H}^{(\mu)}$ on the honeycomb lattice whose matrix element $\mathbf{T}_{\rm H}^{(\mu)}(\boldsymbol{s},\boldsymbol{t})$ is the Boltzmann weight for a spin configuration shown in Fig. 12;

$$\begin{aligned}\mathbf{T}_{\rm H}^{(\mu)}(\boldsymbol{s},\boldsymbol{t}) = \sum_{r_i=\pm 1} & \exp\left[\sum_{m=1}^{M/2} L_3 t_{2m} t_{2m+1}\right] \exp\left[\sum_{m=1}^{M/2} (L_1 r_{2m-1} t_{2m-1} + L_2 r_{2m} t_{2m}\right] \\ & \times \exp\left[\sum_{m=1}^{M/2} L_3 r_{2m-1} r_{2m}\right] \exp\left[\sum_{m=1}^{M/2} (L_1 s_{2m} r_{2m} + L_2 s_{2m-1} r_{2m-1}\right] \\ & \equiv (\mathrm{T}_A \mathrm{T}_{B1} \mathrm{T}_C \mathrm{T}_{B2})(\boldsymbol{s},\boldsymbol{t}).\end{aligned} \tag{B4}$$

The superscript μ $(= 0,1)$ denotes the boundary condition $s_{M+1,j} = (-1)^{\mu} s_{1,j}$. Each of the four factors in the first two lines in Eq. (B4) defines the four matrices T_A, T_{B1}, T_C and T_{B2}, respectively. Their operator forms are

$$\begin{aligned}\mathrm{T}_A &= \prod_{m=1}^{M/2} \exp\left[L_3 \sigma_{2m}^z \sigma_{2m+1}^z\right], \\ \mathrm{T}_{B1} &= \left(\frac{4 z_1 z_2}{k^2}\right)^{M/4} \prod_{m=1}^{M/2} \exp\left[L_1^* \sigma_{2m-1}^x + L_2^* \sigma_{2m}^x\right], \\ \mathrm{T}_{B2} &= \left(\frac{4 z_1 z_2}{k^2}\right)^{M/4} \prod_{m=1}^{M/2} \exp\left[L_2^* \sigma_{2m-1}^x + L_1 * \sigma_{2m}^x\right], \\ \mathrm{T}_C &= \prod_{m=1}^{M/2} \exp\left[L_3 \sigma_{2m-1}^z \sigma_{2m}^z\right],\end{aligned} \tag{B5}$$

where $\boldsymbol{\sigma}_i^{\mu}$ is the Pauli spin operator at site i and $e^{-2L_i^*} = \tanh L_i$. Putting N rows of Fig. 12 in succession and applying the star–triangle transformation gives the $M \times N$ triangular lattice whose basis vectors are rotated by 90^0 from those of Fig. 1(a). Thus, to calculate the toroidal partition function of $T = 0$ TAFIM, we instead carry out the calculation using $\mathbf{T}_{\rm H}^{(\mu)}$. The boundary condition along the vertical direction is $s_{i,N+1} = (-1)^{\nu} s_{i,1}$. For each boundary condition, the partition function $\mathcal{Z}_{\rm TAFIM}^{(\mu,\nu)}$ is written as

$$\mathcal{Z}_{\rm TAFIM}^{(\mu,\nu)} = \mathrm{Tr}\left[\mathbf{T}_{\rm H}^{(\mu)}\right]^N \mathbf{R}^{\nu}, \tag{B6}$$

where $\mathbf{R}$ is the spin-reversal operator.

Following the same procedure as in Ref. [27], we diagonalized the transfer matrix Eq. (B4) exactly. If we write the transfer matrix as $\mathbf{T}_{\rm H}^{(\mu)} = \left(4 z_1 z_2 / k^2\right)^{M/2} e^{-\hat{\mathcal{H}}}$, then the Hamiltonian $\hat{\mathcal{H}}$ after the usual Wigner-Jordan transformation can be written as

$$\hat{\mathcal{H}} = \frac{1}{2} \sum_k \left\{\epsilon_1(k)(2\hat{n}_k - 1) + \epsilon_2(k)(2\hat{m}_k - 1)\right\}, \tag{B7}$$

where $\hat{n}_k$ and $\hat{m}_k$ are the mutually commuting occupation number operators with eigenvalue $n_k, m_k = 0,1$ and $\epsilon_1(k)$ and $\epsilon_2(k)$ are the quasiparticle excitation energy which is given by

$$\begin{aligned}\epsilon_1(k) &= \left|\mathrm{sgn}(k) \cosh^{-1} t_+ - \cosh^{-1} p\right| - i \cos^{-1} t_-, \\ \epsilon_2(k) &= \left|\mathrm{sgn}(k) \cosh^{-1} t_+ + \cosh^{-1} p\right| - i \cos^{-1} t_-,\end{aligned} \tag{B8}$$

where

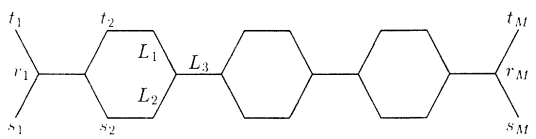

FIG. 12. The honeycomb lattice transfer matrix.

$$t_\pm = \frac{z_3^2}{4z_1z_2} \pm \frac{1}{2}\sqrt{4+\frac{z_3^4}{4z_1^2z_2^2}-\frac{2z_3^2\cos k}{z_1z_2}}, \tag{B9}$$

$$p = \frac{z_1^2+z_2^2}{2z_1z_2} \quad .$$

From now on, we set $z_3 = 1$ since all quantities are functions of z_1/z_3 and z_2/z_3 only. z_i/z_3 in this section is equal to x_i of the text if $\epsilon_i = 0$. [See Eq. (4).] The values of k are restricted to the set

$$k = \frac{2\pi}{M} \times \begin{cases} 2\mathbf{Z} - 1 + \mu & \text{if } \sum_k (n_k + m_k) = \text{ even} \\ 2\mathbf{Z} + \mu & \text{if } \sum_k (n_k + m_k) = \text{ odd} \end{cases} \tag{B10}$$

for boundary condition μ along the horizontal direction.

The partition function $\mathcal{Z}^{(\mu,\nu)}_{\text{TAFIM}}$ is given by

$$\mathcal{Z}^{(\mu,\nu)}_{\text{TAFIM}} = \left(e^{-NE^\mu_e}\mathcal{Z}^\mu_{\text{even}} + (-1)^\nu e^{-NE^\mu_o}\mathcal{Z}^\mu_{\text{odd}}\right) \times \left(\frac{2}{z_3}\right)^{-\mathcal{N}/2}, \tag{B11}$$

where

$$\mathcal{Z}^\mu_{\text{even (odd)}} = \sum_{\text{even (odd)}} \exp\left\{-N\sum_k [\epsilon_1(k)n_k + \epsilon_2(k)m_k]\right\} \quad , \tag{B12}$$

$\sum_{\text{even}}$ ($\sum_{\text{odd}}$) denoting the sums over the occupation number configurations $\{n_k, m_k = 0, 1\}$ under the restriction $\sum_k (n_k + m_k)$ = even (odd), respectively, and the values of k are given in Eq. (B10). We will say a state is in an even (odd) sector if $\sum_k (n_k + m_k)$ is even (odd). In Eq. (B11) E^μ_e and E^μ_o are the ground-state energy in the respective sectors and are given by

$$\begin{aligned} E^\mu_e &= -\frac{1}{2}\sum_{n=1}^{M/2}\left(\epsilon_1\left[\frac{2\pi}{M}(2n-1+\mu)\right] + \epsilon_2\left[\frac{2\pi}{M}(2n-1+\mu)\right]\right) \\ &= -\sum_n \epsilon_1\left[\frac{2\pi}{M}(2n-1+\mu)\right] \\ E^\mu_o &= -\frac{1}{2}\sum_{n=1}^{M/2}\left(\epsilon_1\left[\frac{2\pi(2n+\mu)}{M}\right] + \epsilon_2\left[\frac{2\pi(2n+\mu)}{M}\right]\right) \\ &= -\sum_n \epsilon_1\left[\frac{2\pi(2n+\mu)}{M}\right] \quad . \end{aligned} \tag{B13}$$

We obtain the finite corrections to E^μ_e and E^μ_o from the Euler-Mclaurin formula. The results for periodic boundary condition ($\mu = 0$) are

$$\begin{aligned} E^0_e &= \begin{cases} -\frac{M}{4\pi}\int_0^{2\pi}\epsilon_1(k)dk - \frac{4\pi\epsilon_0'}{M}\left(\frac{1}{12}-\alpha^2\right) & ,\alpha \le \frac{1}{2} \\ -\frac{M}{4\pi}\int_0^{2\pi}\epsilon_1(k)dk - \frac{4\pi\epsilon_0'}{M}\left(\frac{1}{12}-(1-\alpha)^2\right) & ,\alpha \ge \frac{1}{2} \end{cases} \\ E^0_o &= -\frac{M}{4\pi}\int_0^{2\pi}\epsilon_1(k)dk - \frac{4\pi\epsilon_0'}{M}\left(\frac{1}{12}-(1/2-\alpha)^2\right), \end{aligned} \tag{B14}$$

where

$$\epsilon_0' = \left.\frac{d\epsilon_1}{dk}\right|_{k=k_c^+} = \frac{\sqrt{(2z_1^2+2z_2^2-1)-(z_1^2-z_2^2)^2}}{2(z_1^2+z_2^2)-1} \tag{B15}$$

$$\alpha = \frac{k_cM}{4\pi} - \left[\frac{k_cM}{4\pi}\right]$$

with $[x]$ denoting the integer part of x. The ground-state energies for each sector under antiperiodic boundary condition ($\mu = 1$) are

$$E^1_e = E^0_o \quad , \quad E^1_o = E^0_e \quad . \tag{B16}$$

The quantity $\frac{1}{2}\ln(z_3/2) - \frac{1}{4\pi}\int_0^{2\pi}\epsilon_1(k)dk$ is the bulk free energy f_∞ per site.

From the predictions of the conformal-field theory, we know that the transfer matrix has gapless excitations with the linear dispersion relation at the criticality. The quasiparticle excitation energies become zero at $k = \pm k_c$ where

$$\cos k_c = \frac{1}{2z_1z_2}\left[(z_1^2+z_2^2)-(z_1^2-z_2^2)^2\right] \tag{B17}$$

in the range $|z_1 - z_2| \le z_3$ and $|z_1 + z_2| \ge z_3$. So, we conclude that the system is critical in this range. This includes the result of Blöte and Hilhorst [8] who treated the case $z_1 = z_2$.

The toroidal partition function $\tilde{\mathcal{Z}}^{(\mu,\nu)}_{\text{TAFIM}}$ under the general boundary condition (μ, ν) is given as

$$\tilde{\mathcal{Z}}^{(\mu,\nu)}_{\text{TAFIM}} = \lim_{\substack{N,M\to\infty \\ M/N=\text{fixed}}} \mathcal{Z}^{(\mu,\nu)}_{\text{TAFIM}}/e^{-NMf_\infty} \quad . \tag{B18}$$

Especially, the toroidal partition function for periodic boundary condition in both directions is given as

$$\tilde{\mathcal{Z}}^{(0,0)}_{\text{TAFIM}} = \lim_{\substack{N,M\to\infty \\ N/M=\text{fixed}}} e^{\frac{4\pi N}{M}\epsilon_0'(1/12-\alpha^2)}\mathcal{Z}^0_{\text{even}} + e^{\frac{4\pi N}{M}\epsilon_0'[1/12-(1/2-\alpha)^2]}\mathcal{Z}^0_{\text{odd}} \quad . \tag{B19}$$

Since N is large, the modes near $k = \pm k_c$ whose energy scales like $1/M$ contribute factors of $O(1)$ in the sum. Therefore, for $M, N \to \infty$ with N/M fixed, we may replace the dispersion relation by the linear one

$$\epsilon_{1,2}(k) = \epsilon_o'|k \mp k_c| - i\alpha_0'(k - k_c) \mp i\alpha_0, \tag{B20}$$

where

$$\alpha_0' = \left.\frac{d\alpha}{dk}\right|_{k=k_c^+} = \frac{z_2^2 - z_1^2}{2(z_1^2+z_2^2)-1}, \tag{B21}$$

$$\cos\alpha_0 = \cos\alpha(k_c) = \frac{1-z_1^2-z_2^2}{2z_1z_2} \quad .$$

The restricted sums can be done conveniently using the transformation

$$\sum_{\text{even}} = \left[\mathcal{T}_n^e \frac{1}{2}\left\{1+(-1)^{\sum_k n_k}\right\}\right]\left[\mathcal{T}_m^e \frac{1}{2}\left\{1+(-1)^{\sum_k m_k}\right\}\right] + \left[\mathcal{T}_n^e \frac{1}{2}\left\{1-(-1)^{\sum_k n_k}\right\}\right]\left[\mathcal{T}_m^e \frac{1}{2}\left\{1-(-1)^{\sum_k m_k}\right\}\right]$$

$$\sum_{\text{odd}} = \left[\mathcal{T}_n^o \frac{1}{2}\left\{1+(-1)^{\sum_k n_k}\right\}\right]\left[\mathcal{T}_m^o \frac{1}{2}\left\{1-(-1)^{\sum_k m_k}\right\}\right] + \left[\mathcal{T}_n^o \frac{1}{2}\left\{1-(-1)^{\sum_k n_k}\right\}\right]\left[\mathcal{T}_m^o \frac{1}{2}\left\{1+(-1)^{\sum_k m_k}\right\}\right], \quad \text{(B22)}$$

where

$$\mathcal{T}_n^e = \prod_{k=\frac{2\pi}{M}(2n-1)} \sum_{n_k=0,1} \quad \text{and} \quad \mathcal{T}_n^o = \prod_{k=\frac{4\pi n}{M}} \sum_{n_k=0,1}$$

and similarly for $\mathcal{T}_m^e$ and $\mathcal{T}_m^o$.

After a lengthy calculation with this linear dispersion relation Eq. (B20), we obtain

$$\widetilde{\mathcal{Z}}_{\text{TAFIM}}^{(0,0)} = \frac{|\tilde{q}|^{\alpha^2}}{2|\eta(\tilde{q})|^2}\left\{-|\vartheta_1(z,\tilde{q})|^2 + |\vartheta_2(z,\tilde{q})|^2 + |\vartheta_3(z,\tilde{q})|^2 + |\vartheta_4(z,\tilde{q})|^2\right\}, \quad \text{(B23)}$$

where $\eta(q) = q^{1/24}\prod_{n=1}^{\infty}(1-q^n)$ is the Dedekind eta function, ϑ_i are the Jacobi theta function [23], $\tilde{q} = e^{2\pi i\tilde{\tau}}$ with

$$\tilde{\tau} = \frac{2iN}{M}(\epsilon_0' + i\alpha_0')$$

and finally

$$z = \frac{\alpha_0 N}{2} + \pi\alpha\tilde{\tau} \quad .$$

Following the same procedures, we can also calculate $\widetilde{\mathcal{Z}}_{\text{TAFIM}}^{(\mu,\nu)}$ under the general boundary condition (μ,ν). We present only the results.

$$\begin{aligned}
\widetilde{\mathcal{Z}}_{\text{TAFIM}}^{(1,0)} &= \frac{|\tilde{q}|^{\alpha^2}}{2|\eta(\tilde{q})|^2}\left\{|\vartheta_1(z,\tilde{q})|^2 + |\vartheta_2(z,\tilde{q})|^2 + |\vartheta_3(z,\tilde{q})|^2 - |\vartheta_4(z,\tilde{q})|^2\right\}, \\
\widetilde{\mathcal{Z}}_{\text{TAFIM}}^{(0,1)} &= \frac{|\tilde{q}|^{\alpha^2}}{2|\eta(\tilde{q})|^2}\left\{|\vartheta_1(z,\tilde{q})|^2 - |\vartheta_2(z,\tilde{q})|^2 + |\vartheta_3(z,\tilde{q})|^2 + |\vartheta_4(z,\tilde{q})|^2\right\}, \\
\widetilde{\mathcal{Z}}_{\text{TAFIM}}^{(1,1)} &= \frac{|\tilde{q}|^{\alpha^2}}{2|\eta(\tilde{q})|^2}\left\{|\vartheta_1(z,\tilde{q})|^2 + |\vartheta_2(z,\tilde{q})|^2 - |\vartheta_3(z,\tilde{q})|^2 + |\vartheta_4(z,\tilde{q})|^2\right\}.
\end{aligned} \quad \text{(B24)}$$

The toroidal partition function $\widetilde{\mathcal{Z}}_{\text{TAFIM}}^{(\mu,\nu)}$ can be rewritten as an infinite series in $\tilde{q}$. Using the series form of ϑ_i's and rearranging the summands, we obtain

$$\widetilde{\mathcal{Z}}_{\text{TAFIM}}^{(\mu,\nu)} = \frac{1}{|\eta(\tilde{q})|^2}\sum_{n,m\in\mathbf{Z}} (-1)^{\nu} e^{i\alpha_0 N m}\tilde{q}^{[(2n+\mu)/2+\alpha+m/2]^2/2}\,\bar{\tilde{q}}^{[(2n+\mu)/2+\alpha-m/2]^2/2}. \quad \text{(B25)}$$

To compare with the triangular lattice shown in Fig. 1(a), we perform the modular transformation $\tilde{\tau} \to \tau = -1/\tilde{\tau}$. This is achieved by applying Poisson sum formula to both summation indices n and m in Eq. (B25). The resulting expression for the periodic boundary condition $(\mu = 0, \nu = 0)$ is

$$\widetilde{\mathcal{Z}}_{\text{TAFIM}}^{(0,0)} = \frac{1}{|\eta(q)|^2}\sum_{m,n\in\mathbf{Z}} e^{-2\pi i\alpha m} q^{[m/2+(n-\alpha_0 N/2\pi)]^2/2}\bar{q}^{[m/2-(n-\alpha_0 N/2\pi)]^2/2}, \quad \text{(B26)}$$

where $q = e^{2\pi i\tau}$. Note that

$$\tau = \frac{M}{N}\zeta^0 e^{i(\pi-\theta_0)}$$

with

$$\zeta^0 = \left[2(z_1^2+z_2^2)-1\right]^{1/2}/2$$

and

$$\pi - \theta_0 = \cos^{-1}\frac{z_2^2 - z_1^2}{\sqrt{2(z_1^2+z_2^2)-1}}.$$

This is exactly the Coulombic partition function with the twisted boundary conditions and the coupling constant $g = 2$.

Since z_i's are the activities of the diamonds shown in Fig. 1(b), one easily obtains [8] from the bulk free energy that the mean domain-wall densities of each type are given by

$$\langle n_1 + n_2 \rangle / \mathcal{N} = \alpha_0 / \pi, \qquad \langle n_1 - n_2 \rangle / \mathcal{N} = k_c / \pi, \tag{B27}$$

with α_0 and k_c given by Eq. (B21) and (B17), respectively. Therefore, one sees that the twisting angles $\alpha_0 N$ and $-2\pi\alpha$ in Eq. (B26) are related to the total domain-wall densities as

$$\alpha_0 N = \frac{\pi \langle n_1 + n_2 \rangle}{M} \equiv \pi Q_0, \tag{B28}$$

and

$$2\pi\alpha = \frac{\pi \langle n_1 - n_2 \rangle}{N} \equiv \frac{\pi Q_1}{2}, \tag{B29}$$

where Q_0 is the number of domain walls per row and Q_1 is the difference of number of type-1 domain walls and that of type 2 per column. Using these quantities, $\widetilde{\mathcal{Z}}^{(0,0)}_{\mathrm{TAFIM}}$ is written as

$$\widetilde{\mathcal{Z}}^{(0,0)}_{\mathrm{TAFIM}} = \frac{1}{|\eta(q)|^2} \sum_{m,n \in \mathbf{Z}} e^{-i\pi Q_1 m/2} q^{\Delta_{m,n-Q_0/2}(g=2)} \bar{q}^{\Delta_{m,-(n-Q_0/2)}(g=2)} \tag{B30}$$

where $\Delta_{m,n}(g) = \left(m/\sqrt{g} + \sqrt{g}n\right)^2/4$.

[1] P. Bak, Rep. Prog. Phys. **45** , 589 (1982).
[2] F. C. Frank and J. H. Van der Merwe, Proc. R. Soc. **198** , 205 (1949); **198**, 216 (1949).
[3] S. N. Coppersmith, D. S. Fisher, B. I. Halperin, P. A. Lee, and W. F. Brinkman, Phys. Rev. B **25**, 349 (1982).
[4] V. L. Pokrovsky and A. L. Talapov, Phys. Rev. Lett. **42**, 65 (1979).
[5] J. Villian and P. Bak, J. Phys. (Paris) **42**, 657 (1981).
[6] H. Park and M. Widom, Phys. Rev. Lett. **64**, 1076 (1990).
[7] M. D. Grynberg and H. Ceva, Phys. Rev. B **43**, 13 630 (1991).
[8] H. W. J. Blöte and H. J. Hilhorst, J. Phys. A **15**, L631 (1982).
[9] B. Nienhuis, H. J. Hilhorst, and H. W. J. Blöte, J. Phys. A **17**, 3559 (1984).
[10] H. W. J. Blöte, M. P. Nightingale, X. N. Wu, and A. Hoogland, Phys. Rev. B **43**, 8751 (1991).
[11] D. P. Landau, Phys. Rev. B **27**, 5604 (1983).
[12] P. A. Slotte and P. C. Hemmer, J. Phys. C **17**, 4645 (1984).
[13] B. M. Forrest and L.-H. Tang, Phys. Rev. Lett. **64** 1405 (1990).
[14] F. Y. Wu, Phys. Rev. **168**, 539 (1968); E. H. Lieb and F. Y. Wu, *Phase Transitions and Critical Phenomena*, edited by C. Domb and M. S. Green (Academic, New York, 1972).
[15] S. M. Bhattacharjee, Europhys. Lett. **15**, 815 (1991).
[16] F. Y. Wu and H. Kunz (private communication).
[17] M. Gulácsi, H. V. Beijeren, and A. C. Levi, Phys. Rev. E **47**, 2473 (1993).
[18] R. J. Baxter, *Exactly Solved Models in Statistical Mechanics* (Academic, New York, 1982).
[19] Y. A. Izyumov and Y. N. Skryabin, *Statistical Mechanics of Magnetically Ordered System* (Consultants Bureau, New York, 1988).
[20] M. E. Fisher, J. Stat. Phys. **34**, 667 (1984).
[21] J. L. Cardy, Nucl. Phys. **B 270**, 186 (1986); **275**, 200 (1986).
[22] D. Kim and P. A. Pearce, J. Phys. A **20**, L451 (1987).
[23] P. Ginsparg, *Fields, Strings and Critical Phenomena*, edited by E. Brézin and Zinn-Justin (North-Holland, Amsterdam, 1989); P. Di Francesco, H. Saleur, and J.-B. Zuber, Nucl. Phys. B **300**, 393 (1988).
[24] J.-Y. Choi, Ph. D. Thesis, Seoul National University (1990) (unpublished).
[25] H. W. J. Blöte and M. P. Nightingale, Phys. Rev. B **47**, 15046 (1993).
[26] Leh-Hun Gwa and Herbert Spohn, Phys. Rev. A **46**, 844 (1992).
[27] G. H. Wannier, Phys. Rev. **79**, 357 (1950).